JOINT INSTITUTE FOR AERONAUTICS AND ACOUSTICS

NASA
National Aeronautics and Space Administration

Ames Research Center

NASA-CR-169737
19830008967

Stanford University

JIAA TR - 48

EFFECTS OF FLIGHT ON NOISE RADIATED FROM CONVECTED RING SOURCES IN COAXIAL DUAL FLOW

PART 1. THE NOISE FROM UNHEATED JETS

R. Dash

STANFORD UNIVERSITY
Department of Aeronautics and Astronautics
Stanford, California 94305

AUGUST 1982

as the inverted profile incurs a significant massloss and thrustloss. Amongst all the possible coaxial configurations when on of the coaxial streams is heated-conventional profile (CP), inverted profile (IP) and the variable stream control engine (VSCE) cycle-and at constant massflow and thrust, a VSCE-cycle is the most desirable and the best possible engine

ENTER:

DISPLAY 04/2/2

83N17238*# ISSUE 7 PAGE 1089 CATEGORY 71 RPT#: NASA-CR-169737 NAS 1.26:169737 SU-JIAA-TR-48-PT-1 CNT#: NCC2-75 82/08/00 58 PAGES

UNCLASSIFIED DOCUMENT

UTTL: Effects of noise radiated from convected ring sources in coaxial dual flow. Part 1: The noise from unheated jets

AUTH: A/DASH, R.

CORP: Stanford Univ., Calif. CSS: (Joint Inst. for Aeronautics and Acoustics.)

AVAIL.NTIS SAP: HC A04/MF A01

MAJS: /*AIRCRAFT ENGINES/*COAXIAL FLOW/*ENGINE NOISE/*RING STRUCTURES/*SOUND PROPAGATION

MINS: / COAXIAL NOZZLES/ LAMINAR FLOW/ NOISE REDUCTION/ VORTEX SHEETS

ABA: Author

ABS: The effects of flight on sound radiated from embedded, uncorrelated ring sources convecting along the midst of the primary and the secondary streams of a coaxial dual flow which emerges from a moving nozzle into the ambience are studied. Cold jets are examined. The problem is posed as a double vortex-sheet flow model which involves deliberate suppression of

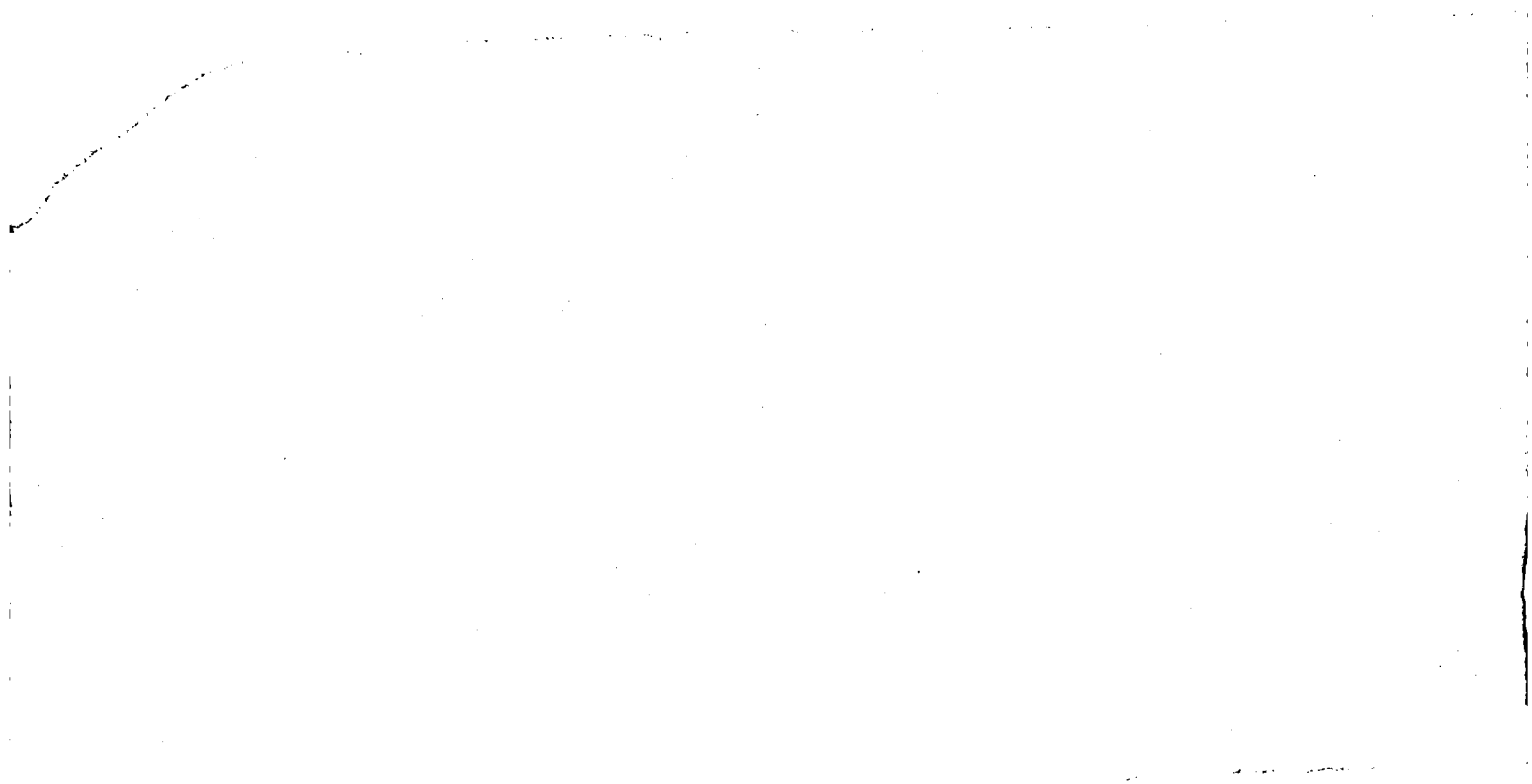

JIAA TR - 48

EFFECTS OF FLIGHT ON NOISE RADIATED FROM CONVECTED RING SOURCES IN COAXIAL DUAL FLOW

Part 1. The Noise From Unheated Jets

R. DASH

The work presented here has been supported by the National Aeronautics and Space Administration under NASA Grant NCC2-75.

TABLE OF CONTENTS

SUMMARY

This paper and its companion work in part 2 study the effects of flight on sound radiated from embedded, uncorrelated ring sources convecting along the midst of the primary and the secondary streams of a coaxial dual flow which emerges from a moving nozzle into the ambience. We examine cold jets here and hot jets in part 2. The problem is posed as a double vortex-sheet flow model which involves deliberate suppression of inherent instabilities of the flow and is formulated, as a linear problem, in terms of the combined contributions of two independent uncorrelated quadrupole-type ring sources, the one convecting in the primary flow representing the sources generated due to the interaction at the primary/secondary interface and the other convecting in the secondary flow representing the sources generated due to the interaction at the secondary/ambient interface. The analysis shows that the effects of flight induce (i) amplification of noise in the forward quadrant, (ii) reduction of noise in the aft quadrant and (iii) absolutely no impact on radiation of noise at $\theta = 90°$ to the jet axis. Moreover, as a result of this study it is inferred (in part 2) that at constant massflow and thrust, the inner-cold/outer-cold mode of operation, although it is not a practical engine cycle, is the quietest mode of operation followed by an inner-hot/outer-hot mode, inner-cold/outer-hot mode and inner-hot/outer-cold mode which radiates the utmost noise. Also it is shown that at constant massflow and thrust, an inverted velocity profile provides a significant noise reduction (as compared against noise from a conventional profile) at all angles both statically and in flight. The salient feature of this study is the simultaneous incorporation of the effects of convection, mean flow and of flight on the radiation from convected sources.

ACKNOWLEDGEMENTS

This study was conducted as part of NASA Ames program of research into flight effects on jet noise under the NASA Co-operative Agreement Contract NCC 2-75. My thanks are due to David H. Hickey and Adolf Atencio of NASA Ames, and K. Karamcheti of Stanford for the benefit of discussion and to Yen Liu of Stanford for his immense help in programming these calculations. My thanks are also extended to Sandra G. Williams of Ames for being so conscientious in her typing.

LIST OF ILLUSTRATIONS

Figure

ABOUT THE CONTRACT AND THE PERSONNEL INVOLVED:

This is a final report covering the period April 1979 to March 1982, and appears in two parts: Part 1 - The Noise From Convected Ring Sources In Coaxial Dual Flow and Part 2 - Effects Of Flight On Noise Radiated From Convected Ring Sources In Coaxial Dual Flow.

This research was carried as part of the aeroacoustics program of the Joint Institute for Aeronautics and Acoustics, Department of Aeronautics and Astronautics, at Stanford University and was sponsored by NASA Ames Research Center under the NASA co-operative Agreement Contract NCC 2-75.

Professor K. Karamcheti, Director of the Institute, was the Principal Investigator of the program and Dr. R. Dash was the Chief Senior Investigator on the program. Professor I. D. Chang and Mr. Yen Liu, a Ph.D. student, also participated in the program. From NASA Ames Research Center Mr. David H. Hickey, Chief of the Low Speed Aircraft Research Branch and Mr. Adolf Atencio, Project Research Engineer, were the technical monitors for this project.

1.1 GENESIS OF THE PROBLEM

The motivation for this work comes from the recent advances in theoretical modelling of jet noise characteristics by Mani (1976a, 1976b), especially the flow-acoustic interaction, which have produced rational explanations for many observed trends in jet noise.

Mani's approach is one of the most simplistic and successful approaches to jet noise problems in recent years. He capitalized on an oversimplified form of a mathematically rigorous, nonlinear, inhomogeneous wave equation originated by Phillips (1960) and developed more fully by Lilley (1972) and Goldstein & Howes (1973). The study with its distinct style by Mani is regarded as a simplified attempt to solve the Lilley-Goldstein & Howes (LGH) type equation where, in the interest of obtaining closed-form solutions and maintaining the clarity of the physics without any recourse to complicating numerical treatment, the jet flow is modelled as a simple, round, plug-flow jet. This is a simplified form of the LGH-equation which is found in the limiting case of a uniform jet surrounded by a infinitely thin vortex sheet. Mani's model succeeds in explaining most major interesting features of jet noise data, on both hot and cold jets. Particular success is achieved in explaining aspects of the data not explainable by the Lighthill approach, especially the flow-acoustic interaction.

In general, many of the experimental features are consistent with the results of the vortex sheet flow model procedure which deliberately suppresses the instability waves that would actually show up in any physical realization being described by that model. Recognizing this general feature of the vortex

sheet flow model and the ease and straightforwardness with which it is handled, Balsa and Gliebe (1977) have extended Mani's theory to explain the noise radiation from coaxial jets. In their work, however, they describe a static jet noise situation and furthermore, by considering just only a single point source at the centerline of a primary jet in a coaxial flow they have failed to provide a right modelling inasmuch as it does not represent all the sources which are generated at the two vortex interfaces.

In a recent work, an extension of the Mani-type vortex sheet flow model, Dash (1978, 1979a, 1979b) has considered the effects of flight to predict the different features associated with the noise from a single stream jet in flight as well as from a coaxial jet in flight. However, the coaxial flow problem there is inadequately modelled since only the acoustic sources due to the primary/secondary flow interactions have been taken into consideration while the acoustic sources due to the secondary/ambient flow interactions have been inadvertently completely ignored.

In the present work, this has been taken care of by considering and including simultaneously the sources both inside the inner jet and inside the outer jet. This is perfectly natural and logical, since in a coaxial flow the interaction between the inner and the outer flows plus the interaction between the outer and the ambient flows inherently give rise to acoustic sources of noise. One has to bear in mind that the sources which are generated due to the interaction of primary/secondary flows are presumed to be axially and symmetrically distributed in and around the primary flow, and as such can be qualitatively represented by considering a ring source convecting in the midst of the primary jet. At the same time, the sources generated due

to the interaction of secondary/ambient flows are presumed to be axially and symmetrically distributed in and around the secondary flow. These sources are qualitatively represented by considering a ring source convecting in the midst of the secondary jet.

The choice for the centerline convection is strongly advocated and also found to have been applied to yield very good results in the works of Mani (1972, 1974, 1976a, 1976b) and his colleaques. This is also supported by the experimental evidence in the work of Scharton and his colleagues (1972). Furthermore, Mani (1974) has also argued that the exact location of the source does not matter so long as it is well within the jet. These ideas help significantly in the handling of mathematics involved in the analysis.

1.2 RELEVANCE OF RING SOURCES IN A VORTEX SHEET FLOW MODEL

It will be interesting to make some remarks about the suitability of considering ring sources in a vortex sheet flow model. It is well known that the vortex sheet flow modelling is a very oversimplified model inasmuch as it deliberately suppresses the instability waves that would actually dominate any physical realization of that model. Nonetheless, incorporation of flow-acoustic interaciton in a vortex sheet model provides many useful results which successfully explain aspects of the jet noise data not explainable by the classical theories. In this context, Ffowcs Williams (1977) has noted that notwithstanding the deliberate suppression of instability waves in a vortex sheet model, the model is so successful that many of the several features recognizable in experimental jet-noise are easily deduced from these model studies.

The inclusion of ring-type sources is appreciated when one understands the basic physics involved in the jet flow phenomenom. In the past few years, several studies have been undertaken which suggest that a large-scale orderly structure lies hidden within the chaotic, noise-producing, tranisiton region of a jet. Using several methods in their study of flow visualization of round jets, Crow and Champagne (1971) have discovered the emergence of an orderly flow pattern, and they have also noticed that at an average Strouhal number of about 0.3 based on frequency, exit speed and diameter, a tenuous train of puffs—rings having axisymmetric structure—is generated in the transitional turbulence region of a jet. These rings are highly structured and stable. The production of doughnut-like rings also finds support in the works of Wooldridge and Wooten (1971). Hardin (1974) has also considered the ring-sources to analyze the noise producing potential of round jets and observes that a noteworthy feature of these studies on the orderly structure of jet turbulence is that these rings may be responsible for most of the jet noise. Crow and Champagne also observe from their previous work on water jets "waves radiating outward from the above region of puff formation". These and several similar inferences of the research workers have prompted the author to include the ring sources in the study of jet noise through the vortex sheet modelling of the flow.

1.3 INDICATION OF THE SCOPE AND METHODS OF APPROACH

The prediction model contains three major elements: i) convection of acoustic sources in the primary flow and in the secondary flow, ii) flow-acoustic interaction due to the above two consituent streams and iii) the effects of flight. Furthermore, all possible combinations of heated and

unheated jets that comprise a coaxial dual flow have also been built into the model.

Analytical discussion is made and explicit radiation results are provided for the three usual types of acoustic sources: monopole, dipole, and quadrupole; however, only the quadrupole type of sources are taken into consideration while theoretically computing the sound production of the coaxial jet flow.

The discussion and analytical development of the model is fully based on the recent works of Mani (1976a, 1976b) who has given a new direction in jet noise theory by casting the whole jet noise problem into the limiting case of a uniform jet surrounded by an infinite vortex sheet. The technique is very clear and will make itself self-explanatory as we proceed with the mathematical development in the following section.

2. SPECIFICATION AND FORMULATION OF THE MODEL

The analysis is intended to model the situation shown in figure 1, in which a coflowing coaxial dual jet exhausts into ambience from a nozzle which is moving in an opposite direction with velocity U_f, which is the velocity of flight. The inner stream of radius r_p, also called the primary stream, is characterized by velocity U_p and the outer stream of radius r_s, also called the secondary stream, is characterized by velocity U_s. Likewise, all the flow parameters—density ρ, speed of sound c, Mach number M and so on and so forth—which are associated with the inner/primary flow are affixed to the suffix (p), and those with the outer/secondary flow are affixed to the suffix (s).

For an observer in a coordinate system fixed to the moving nozzle, it will appear as if he is stationary and the entire ambient world around him is in a state of motion. Consequently, because of this perception it will appear that the whole coaxial dual jet phenomenon is taking place in an ambience which is moving in the same direction as the jet with a speed of motion U_f which is the velocity of flight due to the moving nozzle. Thus the situation could be best simulated in a wind tunnel of which a pictorial model is illustrated in figure 2. The airflow (in the wind tunnel) which surrounds the jet now simulates that which would be created in the case of an otherwise moving aircraft with speed U_f in an actual flow environment.

Consider a cylindrical coordinate system for this plug-flow model where U_p = constant for $0 < r < r_p$ and U_s = constant for $r_p < r < r_s$. As indicated earlier, in what follows we will introduce two ring sources with a suitable choice of their fundamental forms as:

ring in the primary flow: $$q_m \frac{\delta(r-r_o)}{r}\,\delta(z-U_c t)\,e^{i(m\phi-\omega t)}, \quad 0<r_o<r_p \qquad (1$$

Ring in the secondary flow: $$q_n \frac{\delta(r-r_o)}{r}\,\delta(z-\mathcal{U}_c t)\,e^{i(n\phi-\omega t)}, \quad r_p<r_o<r_s \qquad (2$$

where q_m and q_n are constants and reflect the characteristic ring strengths to which we will give proper meaning in due course. These ring sources which are convecting in the midst of the primary and secondary flows would be representative of the axially, symmetrically, distributed sources which arise as a result of flow interaction and exist in and around the primary flows and also the secondary flows. The quantities ω and ω are the frequencies associated with the ring sources in the primary flow and in the secondary flow, and U_c and $\mathcal{U}_c$ are their velocities with which they convect.

At low amplitude the sound waves which are generated due to these sources travel at the same speed regardless of their frequency and as such their propagation in the uniformly flowing fluids (and also in the simulated flow outside the Jet) are described by the following convective inhomogeneous (and also homogeneous) wave equations for pressure p which we write as:

$$\frac{1}{c_p^2}\left(\frac{\partial}{\partial t}+U_p\frac{\partial}{\partial z}\right)^2 p-\nabla^2 p = q_m L_j\left\{\frac{\delta(r-r_0)}{r}\,\delta(z-U_c t)\,e^{i(m\phi-\omega t)}\right\}\cdots$$

inside the primary flow $0\le r\le r_p$

$$\frac{1}{c_s^2}\left(\frac{\partial}{\partial t}+U_s\frac{\partial}{\partial z}\right)^2 p-\nabla^2 p = q_n \mathcal{L}_j\left\{\frac{\delta(r-r_0)}{r}\,\delta(z-\mathcal{U}_c t)\,e^{i(n\phi-\omega t)}\right\}\cdots$$

inside the secondary flow $r_p\le r\le r_s$

$$\frac{1}{c_f^2}\left(\frac{\partial}{\partial t}+U_f\frac{\partial}{\partial z}\right)^2 p-\nabla^2 p = 0\ ,\ \text{inside the simulating flow } r\gg r_s \quad\cdots(5$$

where the differential operators L_j and $\mathcal{L}_j$ are given by:

$$\left.\begin{aligned} &L_1=\mathcal{L}_1=1\\ &L_2=\partial/\partial t+U_p\,\partial/\partial z,\ \mathcal{L}_2=\partial/\partial t+U_s\,\partial/\partial z\\ &L_3=\mathcal{L}_3=\partial/\partial z\\ &L_4=\mathcal{L}_4=\partial^2/\partial z^2 \end{aligned}\right\} \qquad (6)$$

The operators $L_1=\mathcal{L}_1=1$ imply the simple source pulsating nature of the acoustic sources; $L_2=\partial/\partial t+U_p\,\partial/\partial z$ implies the mass fluctuating type ring source in the primary flow and, likewise, $\mathcal{L}_2=\partial/\partial t+U_s\,\partial/\partial z$ also implies another mass fluctuating type ring source in the secondary flow: $L_3=\mathcal{L}_3=\partial/\partial z$ implies an axial dipole-type ring source and $L_4=\mathcal{L}_4=\partial^2/\partial z^2$ implies an axial, longitudinal, quadrupole-type ring source.

The entire problem under consideration is supposed to be perfectly linear and the ring sources in the primary and secondary flows are assumed to be perfectly uncorrelated. Because of the linearity of the equations and the involved boundary conditions, we can consider this as a superposition of two problems, and therefore the resulting radiation effect will be the linear combination of the fields radiated by the ring source in the primary flow and by the ring source in the secondary flow. In view of this we will tackle this problem as two problems side by side—one with a ring source in the primary flow and the other with another ring source in the secondary flow, each source being oblivious of the presence of the other. This is a linear, noninteracting acoustic phenomenom where of course the Laplace equations are linear and the radiation effects are noninteracting due to the uncorrelated nature of the sources involved.

3. MATHEMATICAL DEVELOPMENT AND GENERAL SOLUTION

(Ring-Source in the Secondary Stream)

As indicated earlier we will develop this problem as a combination of two problems. They are a problem of coaxial jet with a ring source in the secondary flow plus a problem of coaxial jet with a ring source in the primary flow. Focussing our attention first to the problem of a coaxial jet flow with a ring source convecting in the secondary flow, without any other type of source being present elsewhere including the primary flow region, one can see that the mathematical problem then involves solving:

$$\left[\frac{1}{c_p^2}\left(\frac{D}{Dt}\right)_p^2 - \nabla^2\right] p = 0 \ , \quad (0 \le r \le r_p) \tag{6}$$

$$\left[\frac{1}{c_s^2}\left(\frac{D}{Dt}\right)_s^2 - \nabla^2\right] p = q_n \mathcal{L}_j \left\{\frac{\delta(r-r_0)}{r}\delta(z-U_c t)\, e^{i(n\phi-\omega t)}\right\}, \quad (r_p \le r \le r_s) \tag{7}$$

$$\left[\frac{1}{c_f^2}\left(\frac{D}{Dt}\right)_f^2 - \nabla^2\right] p = 0 \quad , \quad (r_s \le r) \tag{8}$$

where

$$\left.\begin{aligned}\left(\frac{D}{Dt}\right)_p &= \frac{\partial}{\partial t} + U_p \frac{\partial}{\partial z} \\ \left(\frac{D}{Dt}\right)_s &= \frac{\partial}{\partial t} + U_s \frac{\partial}{\partial z} \\ \left(\frac{D}{Dt}\right)_f &= \frac{\partial}{\partial t} + U_f \frac{\partial}{\partial z}\end{aligned}\right\} \tag{9}$$

The boundary conditions across the primary/secondary flow interface at $r = r_p$ and across the secondary/outer (simulating) flow interface at $r = r_s$ are i) the continuity of acoustic pressure and ii) the continuity of normal particle displacement. The former condition is equivalent to the very commonly used statement: the inner solution is same as the outer solution across the common fluid-interface. The latter condition can be developed from the pressure-displacement relation given as:

$$\begin{aligned}\left(\frac{D}{Dt}\right)_p^2 \eta &= -\frac{1}{\rho_p}\frac{\partial p}{\partial r} \quad , \quad \text{inside the jet} \quad 0 \le r \le r_p \\ \left(\frac{D}{Dt}\right)_s^2 \eta &= -\frac{1}{\rho_s}\frac{\partial p}{\partial r} \quad , \quad \text{inside the jet} \quad r_p \le r \le r_s \\ \left(\frac{D}{Dt}\right)_f^2 \eta &= -\frac{1}{\rho_f}\frac{\partial p}{\partial r} \quad , \quad \text{outside the jet} \quad r_s \le r\end{aligned} \tag{10}$$

Because of the nature of the cold jet where the temperature is everywhere the same as the ambient temperature, we could have easily written $\rho_p = \rho_s = \rho_f$ and also $c_p = c_s = c_f$. This would also facilitate our handling of the involved

mathematics. However, to keep a careful watch as to how each flow stream influences the ultimate noise production, we intentionally wanted to keep the involved parameters of one flow distinct from those of the other flow. Nevertheless, when the actual computation will take place their equivalence will be taken care of to reflect that the results are exclusively for the cold coaxial jet flow only. Another reason for keeping these parameters distinct at this stage is to show how the cold jet results compare with those obtaining from the hot jet, where because of the jet temperature the flow parameters will be different, and also as we will discuss later because of the temperature difference across the boundary, additional source terms will be generated which will influence the overall noise production from the coaxial jet.

Before we introduce the Fourier transformation into the equations, with respect to z-coordinate, we note that since

$$\delta(z-\mathcal{U}_c t)=\frac{1}{2\pi}\int e^{ik_3(z-\mathcal{U}_c t)}\,dk_3 \tag{11}$$

the right hand side source term in equation (7) is given by:

$$q_n\ \mathcal{L}_j\left\{\frac{\delta(r-r_0)}{r}\int_{-\infty}^{\infty}\exp i\left[(k_3 z+n\phi)-(\omega+k_3\mathcal{U}_c)t\right]dk_3\right\} \tag{12}$$

As we know the expression (12) is the driving term in the whole problem and as such the ϕ, z, t dependence of all quantities in the Fourier transform formulation will be $\sim \exp i[(k_3 z + n\phi) - (\omega + k_3 \mathcal{U}_c)t]$. This is due to the fact that on a linear theory a term proportional to e^{ikx} in the forcing effect elicits responses proportional to e^{ikx} everywhere in the system whereby the corresponding values of the acoustic pressure, velocity, displacement, potential or any other acoustic parameter are themselves proportional to e^{ikx}. In view of this the Fourier transforms of the pressure and displacement terms are defined as:

$$p(r,\phi,z,t) = \int_{-\infty}^{\infty} \tilde{p}(r,k_3) \exp i\left[(k_3 z + n\phi) - (\omega + k_3 \mathcal{U}_c)t\right] dk_3 \qquad (13)$$

$$\eta(r,\phi,z,t) = \int_{-\infty}^{\infty} \tilde{\eta}(r,k_3) \exp i\left[(k_3 z + n\phi) - (\omega + k_3 \mathcal{U}_c)t\right] dk_3 \qquad (14)$$

Introducing equations (13)-(14), and making use of the Laplacian operator

$$\nabla^2 = \frac{\partial^2}{\partial r^2} + \frac{1}{r}\frac{\partial}{\partial r} + \frac{1}{r^2}\frac{\partial^2}{\partial \phi^2} + \frac{\partial^2}{\partial z^2} \qquad (15)$$

in equations (6-8), one obtains

$$\left(\frac{\partial^2}{\partial r^2} + \frac{1}{r}\frac{\partial}{\partial r} + \mathcal{K}_p^2 - \frac{n^2}{r^2}\right)\tilde{p} = 0 \quad , \text{ for } \quad 0 \le r \le r_p \qquad (16)$$

$$\left(\frac{\partial^2}{\partial r^2} + \frac{1}{r}\frac{\partial}{\partial r} + \mathcal{K}_s^2 - \frac{n^2}{r^2}\right)\tilde{p} = q_n \frac{\delta(r-r_0)}{2\pi r}\mathcal{K}_j(k_3) \quad , \qquad (17)$$

$$\text{for } r_p \le r \le r_s$$

$$\left(\frac{\partial^2}{\partial r^2}+\frac{1}{r}\frac{\partial}{\partial r}+\mathcal{K}_f^2-\frac{n^2}{r^2}\right)\tilde{P}=0\ ,\quad \text{for}\quad r_s\le r \tag{18}$$

where

$$\left.\begin{aligned}\mathcal{K}_p^2&=\left(\frac{c_o}{c_p}\right)^2\left[k+(M_c-M_p)k_3\right]^2-k_3^2\\ \mathcal{K}_s^2&=\left(\frac{c_o}{c_s}\right)^2\left[k+(M_c-M_s)k_3\right]^2-k_3^2\\ \mathcal{K}_f^2&=\left(\frac{c_o}{c_f}\right)^2\left[k+(M_c-M_f)k_3\right]^2-k_3^2\end{aligned}\right\} \tag{19}$$

$$\left.\begin{aligned}&\mathcal{K}_1=-1,\quad \mathcal{K}_2=ic_o\left[k+(M_c-M_s)k_3\right]\\ &\mathcal{K}_3=-ik_3,\quad \mathcal{K}_4=k_3^2,\quad k=\omega/c_o\end{aligned}\right\} \tag{20}$$

$$M_p=U_p/c_o\ ,\quad M_s=U_s/c_o\ ,\quad M_f=U_f/c_o\ ,\quad M_c=\mathcal{U}_c/c_o \tag{21}$$

It has to be pointed out that the $\mathcal{K}_j$'s have been obtained by transferring the $\mathcal{L}_j$'s, and therefore the solutions associated with $\mathcal{K}_1$ represent the pulsating monoploe type effects due to the ring source; the solutions associated with $\mathcal{K}_2$ represent the mass fluctuation type effects; those associated with $\mathcal{K}_3$ represent the axial dipole type effects; and those associated with $\mathcal{K}_4$ represent the axial longitudinal quadrupole type effects. The quantities M_p, M_s, etc. are strictly speaking the normalized velocities, although we refer them here quite often as the flow Mach numbers. Making use of the relations (13)-(14) in equation (10), one can write down the boundary conditions of continuity of normal particle displacement on $r = r_p$, and on $r = r_s$ respectively as:

$$\left(\rho_p/\rho_s\right)\left[\frac{k+(M_c-M_p)k_3}{k+(M_c-M_s)k_3}\right]^2\left(\frac{\partial\tilde{p}}{\partial r}\right)_{r_p(+)}=\left(\frac{\partial\tilde{p}}{\partial r}\right)_{r_p(-)} \tag{22}$$

$$\left(\rho_s/\rho_f\right)\left[\frac{k+(M_c-M_s)k_3}{k+(M_c-M_f)k_3}\right]^2\left(\frac{\partial\tilde{p}}{\partial r}\right)_{r_s(+)}=\left(\frac{\partial\tilde{p}}{\partial r}\right)_{r_s(-)} \tag{23}$$

The propagation constants, $\mathcal{K}_f^2, \mathcal{K}_s^2, \mathcal{K}_p^2$ may be either positive or negative; however, in order that the solution in the outermost simulating ambient medium $r_s \leqslant r$ has to be a solely propagating type $\mathcal{K}_f$ must always be positive in character i.e. $\mathcal{K}_f > 0$. Since the other two propagating constants $\mathcal{K}_s^2$ and $\mathcal{K}_p^2$ describe the wave propagation inside the outer and inner flows respectively, they can be either +ve or -ve. However, we will write down the general solution for (16)-(18) for one of these four possible cases-i.e. when $\mathcal{K}_p, \mathcal{K}_s, \mathcal{K}_f > 0$:

$$\tilde{p}(r,\mathcal{K}_p)=\mathcal{D}_n J_n(\mathcal{K}_p r)\quad,\quad \text{for}\quad 0\leq r\leq r_p \tag{24}$$

$$\tilde{p}(r,\mathcal{K}_s)=\mathcal{B}_n J_n(\mathcal{K}_s r)+\mathcal{C}_n Y_n(\mathcal{K}_s r)+\frac{q_n}{4i}\mathcal{K}_j(k_3)\mathcal{F}_n\,,\quad \text{for}\quad r_p\leq r\leq r_s \tag{25}$$

$$\tilde{p}(r,\mathcal{K}_f)=\mathcal{A}_n H_n(\mathcal{K}_f r)\,,\quad \text{for}\quad r_s\leq r \tag{26}$$

$$\mathcal{F}_n=\left\{\begin{array}{l} J_n(\mathcal{K}_s r)H_n(\mathcal{K}_s r_0)\,,\ \text{for}\ r\leq r_0 \\ J_n(\mathcal{K}_s r_0)H_n(\mathcal{K}_s r)\,,\ \text{for}\ r\geqslant r_0 \end{array}\right\} \tag{27}$$

Now making use of the boundary conditions, as defined in the paragraph preceding equation (10) and also as mathematically expressed in equations (22) and (23), one can obtain from the foregoing equations in (24)-(27) a solution for the outgoing field as:

$$\left.\begin{aligned} \tilde{P}(r, \mathcal{K}_f) &= \mathcal{A}_n H_n(\mathcal{K}_f r) \;, \quad r_s \le r \\ \mathcal{A}_n &= \frac{q_n}{2\pi r_s} \mathcal{K}_j(k_3) \frac{J_n(\mathcal{K}_s r_o)\mathcal{G}_{sp}(Y_n, J_n) - Y_n(\mathcal{K}_s r_o)\mathcal{G}_{sp}(J_n, J_n)}{\mathcal{G}_{fs}(H_n, J_n)\mathcal{G}_{sp}(Y_n, J_n) - \mathcal{G}_{fs}(H_n, Y_n)\mathcal{G}_{sp}(J_n, J_n)} \end{aligned}\right\} \quad (28)$$

where,

$$\mathcal{G}_{sp}(Y_n, J_n) = \mathcal{K}_s \mathcal{M}_{ps} Y_n'(\mathcal{K}_s r_p) J_n(\mathcal{K}_p r_p) - \mathcal{K}_p Y_n(\mathcal{K}_s r_p) J_n'(\mathcal{K}_p r_p) \quad (29)$$

$$\mathcal{G}_{sp}(J_n, J_n) = \mathcal{K}_s \mathcal{M}_{ps} J_n'(\mathcal{K}_s r_p) J_n(\mathcal{K}_p r_p) - \mathcal{K}_p J_n(\mathcal{K}_s r_p) J_n'(\mathcal{K}_p r_p) \quad (30)$$

$$\mathcal{G}_{fs}(H_n, J_n) = \mathcal{K}_f \mathcal{M}_{sf} H_n'(\mathcal{K}_f r_s) J_n(\mathcal{K}_s r_s) - \mathcal{K}_s H_n(\mathcal{K}_f r_s) J_n'(\mathcal{K}_s r_s) \quad (31)$$

$$\mathcal{G}_{fs}(H_n, Y_n) = \mathcal{K}_f \mathcal{M}_{sf} H_n'(\mathcal{K}_f r_s) Y_n(\mathcal{K}_s r_s) - \mathcal{K}_s H_n(\mathcal{K}_f r_s) Y_n'(\mathcal{K}_s r_s) \quad (32)$$

$$\mathcal{M}_{ps} = (\rho_p/\rho_s)\left[\frac{k + (\mathcal{M}_c - M_p)k_3}{k + (\mathcal{M}_c - M_s)k_3}\right]^2 \quad (33)$$

$$\mathcal{M}_{sf} = (\rho_s/\rho_f)\left[\frac{k + (\mathcal{M}_c - M_s)k_3}{k + (\mathcal{M}_c - M_f)k_3}\right]^2 \quad (34)$$

J_n and Y_n are the Bessel functions of the first kind and of the second kind of order n; H_n (same as $H_n^{(1)}$) is called the Bessel function of the third kind, also called the Hankel function, of order n. Dashes denote differentiation with respect to the argument. It is worthwhile to note that solution in equation (28) is developed for the case when all the propagation constants $\mathcal{K}_p^2, \mathcal{K}_s^2, \mathcal{K}_f^2 > 0$. There may arise some cases when either $\mathcal{K}_p^2 < 0$ or $\mathcal{K}_s^2 < 0$; or both $\mathcal{K}_p^2 < 0$ and $\mathcal{K}_s^2 < 0$ simultaneously. In such cases one can write, $\mathcal{K}_p^2 = -\mathcal{K}_p'^2$ or $\mathcal{K}_s^2 = -\mathcal{K}_s'^2$, so that $\mathcal{K}_p = i\mathcal{K}_p'$ and $\mathcal{K}_s = i\mathcal{K}_s'$. Then making use of the Bessel relations $J_n(ix) = i^n I_n(x)$ and $H_n(ix) = (2/\pi)\frac{K_n(x)}{i^{n+1}}$ in equations (28)-(32), one can easily find the appropriate solution for any of these four possible cases. However, either way one finds the same results whether through the above Bessel replacements or working through the individual cases by considering their fundamental results and applying the matching conditions at the boundaries at $r = r_p$ and at $r = r_s$.

As indicated earlier, for the waves to be outgoing we must have $\mathcal{K}_f^2 > 0$ which yields:

$$-\frac{k}{c_f c_0 + (Mc - M_f)} \leq k_3 \leq \frac{k}{c_f/c_0 - (Mc - M_f)} \tag{35}$$

This inequality determines the range of k_3 which ensures a propagating type solution of the radiation problem.

3.1 RADIATION IN THE FAR-FIELD

Now to transform the acoustic pressure in equation (28) in Fourier space to a corresponding one in physical space we make use of equation (13) to write:

$$\tilde{p}(r,\phi,z,t) = \int_{-\infty}^{\infty} \mathcal{A}_n H_n(\mathcal{K}_f r) \exp i\left[(k_3 z + n\phi) - (\omega + k_3 \mathcal{U}_c)t\right] dk_3 \tag{36}$$

Evaluation of the above integral is prohibitively difficult because of the involved, complicating expression for $\mathcal{A}_n$ (see equation (28)). Thus, unless one resorts to direct numerical integration, one should apply the method of stationary phase to find the far-field radiation which is incidentally of prime interest to us. Without going through the details of this method, we may derive the far-field expression for p as:

$$p(R,\theta,\phi,t) = \frac{2}{iR} \frac{\mathcal{A}_n(k_3)_0 \exp i\{R k c_0/c_f - \omega t\}}{\left[1 - c_0/c_f (M_c - M_f)\cos\theta\right]} e^{in(\phi - \pi/2)}$$

$$= \frac{q_n}{i\pi r_s} \frac{\mathcal{K}_j(k_3)_0 \cdot E_n}{R} \frac{\exp i\{R k c_0/c_f - \omega t + n(\phi - \pi/2)\}}{\left[1 - c_0/c_f (M_c - M_f)\cos\theta\right]} \tag{37}$$

where E_n and the stationary point $(k_3)_0$ are given by:

$$E_n = \frac{J_n(\mathcal{K}_s r_0)\, \mathcal{G}_{sp}(Y_n, J_n) - Y_n(\mathcal{K}_s r_0)\, \mathcal{G}_{sp}(J_n, J_n)}{\mathcal{G}_{fs}(H_n, J_n)\, \mathcal{G}_{sp}(Y_n, J_n) - \mathcal{G}_{fs}(H_n, Y_n)\, \mathcal{G}_{sp}(J_n, J_n)} \tag{38}$$

$$(k_3)_o = \frac{k\, c_o/c_f \cos\theta}{[1 - c_o/c_f (\mathcal{M}_c - M_f)\cos\theta]} \tag{39}$$

In view of the stationary point value in equation (39), we now redefine our involved terms in equations (19)-(20), and in equations (33)-(34) as:

$$\mathcal{K}_p = \frac{k}{1 - c_o/c_f (\mathcal{M}_c - M_f)\cos\theta}\left\{\left(\frac{c_o}{c_p}\right)^2\left[1 - c_o/c_f (M_p - M_f)\cos\theta\right]^2 - \left(c_o/c_f \cos\theta\right)^2\right\}^{1/2}$$

$$\mathcal{K}_s = \frac{k}{1 - c_o/c_f (\mathcal{M}_c - M_f)\cos\theta}\left\{\left(\frac{c_o}{c_s}\right)^2\left[1 - c_o/c_f (M_s - M_f)\cos\theta\right]^2 - \left(c_o/c_f \cos\theta\right)^2\right\}^{1/2}$$

$$\mathcal{K}_f = \frac{k\, c_o/c_f \sin\theta}{1 - c_o/c_f (\mathcal{M}_c - M_f)\cos\theta} \tag{40}$$

$$\left.\begin{aligned}
&\mathcal{K}_1 = -1, \quad \mathcal{K}_2 = i c_o k \left[\frac{1 - c_o/c_f (M_s - M_f)\cos\theta}{1 - c_o/c_f (\mathcal{M}_c - M_f)\cos\theta}\right] \\
&\mathcal{K}_3 = -ik\, c_o/c_f \frac{\cos\theta}{[1 - c_o/c_f (\mathcal{M}_c - M_f)\cos\theta]} \\
&\mathcal{K}_4 = \frac{(k\, c_o/c_f)^2 \cos^2\theta}{[1 - c_o/c_f (\mathcal{M}_c - M_f)\cos\theta]}
\end{aligned}\right\} \tag{41}$$

$$\mathcal{N}_{ps} = \left(\rho_p/\rho_s\right)\left[\frac{1 - c_o/c_f (M_p - M_f)\cos\theta}{1 - c_o/c_f (M_s - M_f)\cos\theta}\right]^2 \tag{42}$$

$$\mathcal{N}_{sf} = \left(\rho_s/\rho_f\right)\left[1 - c_o/c_f (M_s - M_f)\cos\theta\right]^2 \tag{43}$$

The quantity c_0/c_f is the ratio of the speed of sound in an ambient quiescent reference fluid (at the normal temperature and pressure conditions of the atmosphere) to the speed of sound in the external fluid through which the propagation of acoustic waves actually takes place. It has to be pointed out that c_0/c_f is retained to show as to what extent the pressure field can be influenced when the external fluid is completely different from the hypothetically quiescent reference fluid. For example the actual atmosphere may be gusty, turbulent, hot etc.etc, so that $c_0/c_f \neq 1$. However, in our final computation we preferred to take $c_0/c_f = 1$ in generating the plots to explain the sound production of the cold coaxial jet.

$\mathcal{R}$ and θ are as shown in Figure 3. Whereas $\mathcal{R}$ is the distance between the center of the ring source and the observer's location, θ is the angle made by the line joining them and the direction of source convection, all at the time of emission. In other words, $\mathcal{R}$ and θ are the retarded co-ordinates. It has to be pointed out here that the equation (37) embodies the field generated due to any type of ring source—monopole, dipole or quadruple—because of the presence of $\mathcal{K}_j$ (k_3) which defines the source characteristics according as $j = 1,2,3,$ or 4. We shall make use of all these at a later stage when we make the calculation of the effective pressure field.

3.2 FAR-FIELD LOW FREQUENCY ANALYSIS

In analyzing the low frequency radiation of the pressure field, we make use of the limiting forms of Bessel and Hankel functions for small arguments, when ν is fixed and $z \to 0$:

$$\left.\begin{aligned} J_\nu(z) &\sim \left(z/2\right)^\nu \Big/ \Gamma(\nu+1) \\ Y_\nu(z) &\sim -i\, H_\nu^{(1)}(z) \sim -\left(\frac{1}{\pi}\right)\Gamma(\nu)\Big/\left(z/2\right)^\nu \end{aligned}\right\} \qquad (44)$$

When we think of a low frequency analysis, we can well impose the restrictions that kr_p, kr_s, and $kr_0 \sim 0$ so that the equations in (29)-(32) are reduced to

$$\mathcal{G}_{sp}(Y_n, J_n) \sim \frac{1}{\pi r_p}\left(\frac{\mathcal{K}_p}{\mathcal{K}_s}\right)^n \left[\mathcal{U}_{ps}+1\right] \tag{45}$$

$$\mathcal{G}_{sp}(J_n, J_n) \sim \frac{(\mathcal{K}_s \mathcal{K}_p)^n}{r_p}\left(r_p/2\right)^n \frac{\left[\mathcal{U}_{ps}-1\right]}{\Gamma(n)\Gamma(n+1)} \tag{46}$$

$$\mathcal{G}_{fs}(H_n, J_n) \sim -\frac{1}{\pi i r_s}\left(\frac{\mathcal{K}_s}{\mathcal{K}_f}\right)^n \left[\mathcal{U}_{sf}+1\right] \tag{47}$$

$$\mathcal{G}_{fs}(H_n, Y_n) \sim \left(\frac{1}{\mathcal{K}_f \mathcal{K}_s}\right)^n \left(\frac{2}{r_s}\right)^{2n} \frac{\Gamma(n)\Gamma(n+1)}{\pi^2 i r_s}\left[\mathcal{U}_{sf}-1\right] \tag{48}$$

Making use of the foregoing relations in equation (38), one can derive from equation (37), a low frequency far field solution for the ring source in the secondary fluid as follows:

$$p(R,\theta,\phi,t) = -\frac{q_n \mathcal{K}_j (k_3)_0}{\Gamma(n+1)}\left(\frac{\mathcal{K}_f r_0}{2}\right)^n \cdot \left[\frac{(\mathcal{U}_{ps}+1)+(\mathcal{U}_{ps}-1)\left(r_p/r_0\right)^{2n}}{(\mathcal{U}_{sf}+1)(\mathcal{U}_{ps}+1)+(\mathcal{U}_{sf}-1)(\mathcal{U}_{ps}-1)\left(r_p/r_s\right)^{2n}}\right] \cdot \frac{\exp i\left\{Rk\, c/c_f - \omega t + n(\phi-\pi/2)\right\}}{R\left[1-c/c_f\,(\mathcal{M}_c - M_f)\cos\theta\right]} \tag{49}$$

The quantity kr_0 is implicit in $\mathcal{K}_f r_0$ and is itself a small quantity because of the low frequency nature of the source. The use of the inequalities, $r_p/r_0 < 1$ and $r_p/r_s < 1$, in the above yields

$$\lim_{n\to\infty}\left|\frac{p_{n+1}}{p_n}\right| \to 0 \tag{50}$$

where p_n is the pressure due to the ring source having periodicity n along ϕ which occurs in the form of $e^{in\phi}$. Thus as shown above one can infer that:

$$|p_0| > |p_1| > |p_2| > \cdots \cdots > |p_n| > |p_{n+1}| > \cdots \cdots \tag{51}$$

This merely tells that as the mode n along ϕ increases, the radiation due to the source decreases and eventually becomes vanishingly small as $n \to \infty$. This also implies that the most powerful radiation comes when the ring is without any periodicity along ϕ -direction in which case the ring turns out to be an axisymmetric doughnut type ring which finds support in the works Crow and Champagne (1971), Wooldridge and Wooten (1971) and in that of Hardin (1974). This decreasing character of source radiation as n increases is not at all surprising if one thinks of the physical nature of the rings with high periodicity. What happens in this case is that positive and negative parts effectively cancel each other out as n goes on increasing. This is evident from Figure 4.

Thus in our subsequent analysis we will consider only axisymmetric rings without any periodicity along ϕ, so that the factor involving $e^{in\phi}$ will be completely absent in all the mathematical expressions to follow. It will be of interest to know that if we make n = 0 in equation (49), the low frequency (far field) radiation is reduced to:

$$p(R,\theta,\phi,t) = -\frac{2q_0\,\mathcal{K}_j(k_3)_0\,\mathcal{U}_{ps}}{\left[(\mathcal{U}_{sf}+1)(\mathcal{U}_{ps}+1)+(\mathcal{U}_{sf}-1)(\mathcal{U}_{ps}-1)\right]}\cdot$$

$$\frac{\exp i\{Rk\,c_0/c_f - \omega t\}}{R\left[1-c_0/c_f(\mathcal{U}_c - M_f)\cos\theta\right]} \qquad (52)$$

and that this is obtained as a result of a drastic approximation where the arguments in the Bessel functions tend to zero. This approximation embodies the product $k\mathcal{R}_0$ (and kr_p, kr_s) which also tend to zero. However, while dealing with the far-field radiation in the following section we will make use of the equation (37) which is exact in frequency.

3.3 FAR-FIELD INTENSITY DUE TO THE RING-SOURCE IN THE SECONDARY STREAM

To predict the intensity of radiation due to the source in the secondary stream, the fundamental solutions associated with various quadrupoles must be employed in a specific manner to represent the radiation pattern due to an axially symmetric sound field. The works of Ribner(1969) and Mani(1976a, 1976b) suggest that the acoustic contribution may be evaluated from the formula

I_{rcs} = Far-Field intensity due to a ring-source in the cold secondary-stream

$$\propto \sum_{i,j=1}^{3} \langle \bar{a}_{ij}^2 \rangle \qquad (53)$$

Here $\langle \bar{a}_{ij}^2 \rangle$ is used to represent the circumferential average of the mean square value of the enclosed quantity, where we express mathematically

$$\langle \bar{a}_{ij}^2 \rangle = \frac{1}{2\pi}\int_0^{2\pi} \bar{a}_{ij}^2 \, d\phi \quad , \quad \bar{a}_{ij}^2 = (a_{ij})(a_{ij})^* \tag{54}$$

The suffixes in equations (53) and (54) characterize the type of quadrupole, and the star above implies its complex conjugate. To find out the radiation due to all the quadrupole components to be made use of in equation (53), we need to find some more related terms. Making use of equations (37) for an axisymmetric ring source without any periodicity n along ϕ (i. e., n = 0), and differntiating the simple source result with respect to the source co-ordinate at $r = r_0$, one can write:

$$\left(\frac{\partial p}{\partial r}\right)_{r_0} = -\frac{\rho_s \mathcal{K}_1}{i\pi r_s} \mathcal{K}_s C_1 \frac{\exp i\{Rk c_0/c_f - \omega t\}}{R[1 - c_0/c_f(M_c - M_f)\cos\theta]} \tag{55}$$

$$\left(\frac{\partial^2 p}{\partial r^2}\right)_{r_0} = -\frac{\rho_s \mathcal{K}_1}{i\pi r_s} \frac{\mathcal{K}_s^2 (C_0 - C_2)}{2} \frac{\exp i\{Rk c_0/c_f - \omega t\}}{R[1 - c_0/c_f(M_c - M_f)\cos\theta]} \tag{56}$$

$$\left(\frac{\partial^2 p}{\partial r \partial z}\right)_{r_0} = -\frac{\rho_s \mathcal{K}_3}{i\pi r_s} \mathcal{K}_s C_1 \frac{\exp i\{Rk c_0/c_f - \omega t\}}{R[1 - c_0/c_f(M_c - M_f)\cos\theta]} \tag{57}$$

where we have,

$$C_0 = \frac{J_0(\mathcal{K}_s r_0)\mathcal{G}_{sp}(Y_0, J_0) - Y_0(\mathcal{K}_s r_0)\mathcal{G}_{sp}(J_0, J_0)}{\mathcal{G}_{fs}(H_0, J_0)\mathcal{G}_{sp}(Y_0, J_0) - \mathcal{G}_{fs}(H_0, Y_0)\mathcal{G}_{sp}(J_0, J_0)} \tag{58}$$

$$C_1 = \frac{J_1(\mathcal{K}_s r_0)\mathcal{G}_{sp}(Y_0, J_0) - Y_1(\mathcal{K}_s r_0)\mathcal{G}_{sp}(J_0, J_0)}{\mathcal{G}_{fs}(H_0, J_0)\mathcal{G}_{sp}(Y_0, J_0) - \mathcal{G}_{fs}(H_0, Y_0)\mathcal{G}_{sp}(J_0, J_0)} \tag{59}$$

$$C_2 = \frac{J_2(\mathcal{K}_s r_0)\mathcal{G}_{sp}(Y_0, J_0) - Y_2(\mathcal{K}_s r_0)\mathcal{G}_{sp}(J_0, J_0)}{\mathcal{G}_{fs}(H_0, J_0)\mathcal{G}_{sp}(Y_0, J_0) - \mathcal{G}_{fs}(H_0, Y_0)\mathcal{G}_{sp}(J_0, J_0)} \tag{60}$$

In deriving equations (55-57) from equation (37), we consider the source strength of the ring as directly proportional to the density of the fluid in which the source is located, so that we replace q_0 by $_s$ which is the density of the secondary stream. Now introducing the following coordinate relations for an axisymmetric ring source devoid of any periodicity n along ϕ,

$$\frac{\partial}{\partial x} = \cos\phi \frac{\partial}{\partial r} \quad , \quad \frac{\partial}{\partial y} = \sin\phi \frac{\partial}{\partial r}$$

$$\frac{\partial^2}{\partial x^2} = \cos^2\phi \frac{\partial^2}{\partial r^2} + \frac{\sin^2\phi}{r} \frac{\partial}{\partial r}$$

$$\frac{\partial^2}{\partial y^2} = \sin^2\phi \frac{\partial^2}{\partial r^2} + \frac{\cos^2\phi}{r} \frac{\partial}{\partial r}$$

$$\frac{\partial^2}{\partial x \partial y} = \cos\phi \sin\phi \frac{\partial^2}{\partial r^2} - \cos\phi \sin\phi \frac{\partial}{\partial r}$$

$$\frac{\partial^2}{\partial y \partial z} = \sin\phi \frac{\partial^2}{\partial r \partial z}$$

$$\frac{\partial^2}{\partial x \partial z} = \cos\phi \frac{\partial^2}{\partial r \partial z} \qquad (61)$$

and making use of the relations in equations (37, 55-57) one can find out the radiation due to all the fundamental quadrupole components which can be written as follows:

$$a_{11} = \frac{\rho_s \mathcal{K}_s}{i\pi r_s h_o}\left[\frac{\mathcal{K}_s h_o (C_o - C_2)}{2}\cos^2\phi + C_1 \sin^2\phi\right]\frac{\exp i\{\mathcal{R}k c_o/c_f - \omega t\}}{\mathcal{R}[1 - c_o/c_f(M_c - M_f)\cos\theta]}$$

$$a_{22} = \frac{\rho_s \mathcal{K}_s}{i\pi r_s h_o}\left[\frac{\mathcal{K}_s h_o (C_o - C_2)}{2}\sin^2\phi + C_1 \cos^2\phi\right]\frac{\exp i\{\mathcal{R}k c_o/c_f - \omega t\}}{\mathcal{R}[1 - c_o/c_f(M_c - M_f)\cos\theta]}$$

$$a_{33} = \frac{\rho_s}{i\pi r_s}(k c_o/c_f)^2 \cos^2\theta \cdot C_o \cdot \frac{\exp i\{\mathcal{R}k c_o/c_f - \omega t\}}{\mathcal{R}[1 - c_o/c_f(M_c - M_f)\cos\theta]^3}$$

$$a_{12} = \frac{\rho_s \mathcal{K}_s}{i\pi r_s h_o}\sin\phi\cos\phi\left[\frac{\mathcal{K}_s h_o (C_o - C_2)}{2} - C_1\right]\frac{\exp i\{\mathcal{R}k c_o/c_f - \omega t\}}{\mathcal{R}[1 - c_o/c_f(M_c - M_f)\cos\theta]}$$

$$a_{13} = \frac{\rho_s \mathcal{K}_s}{\pi r_s} k c_o/c_f \cos\theta\cos\phi \cdot \frac{C_1 \exp i\{\mathcal{R}k c_o/c_f - \omega t\}}{\mathcal{R}[1 - c_o/c_f(M_c - M_f)\cos\theta]^2}$$

$$a_{23} = \frac{\rho_s \mathcal{K}_s}{\pi r_s} k c_o/c_f \cos\theta\sin\phi \cdot \frac{C_1 \exp i\{\mathcal{R}k c_o/c_f - \omega t\}}{\mathcal{R}[1 - c_o/c_f(M_c - M_f)\cos\theta]^2} \tag{62}$$

Using the above relations in equation (54), the far field radiation given by the formula in equation (53) yields:

$$\begin{aligned} I_{rcs} &= \langle \bar{a}_{33}^2 \rangle + 2\langle \bar{a}_{11}^2 \rangle + 2\langle \bar{a}_{12}^2 \rangle + 4\langle \bar{a}_{13}^2 \rangle \\ &= \left(\frac{\rho_s}{\pi \mathcal{R} r_s h_o}\right)^2 \frac{1}{Q_2^2 |\delta_2|^2}\left\{\frac{|\gamma_0|^2 \lambda_{3s}^2 (c_o/c_f)^4 \cos^4\theta}{Q_2^2 |M_2|^2}\right. \\ &+ \left|\frac{3}{16}[\chi_2(\gamma_0 - \gamma_2)]^2 + \frac{3}{4}\gamma_1^2 + \frac{\chi_2\gamma_1}{4}(\gamma_0 - \gamma_2)\right| \\ &+ \left|\frac{1}{16}[\chi_2(\gamma_0 - \gamma_2)]^2 + \frac{\gamma_1^2}{4} - \frac{\chi_2\gamma_1}{4}(\gamma_0 - \gamma_2)\right| \\ &\left. + \frac{2|\gamma_1|^2 \lambda_{3s}^2 (c_o/c_f)^2 \cos^2\theta}{Q_2^2}\right\} \end{aligned} \tag{63}$$

where

$$\delta_2 = E\beta_0\ J_0(u_2) + \alpha_0\ J_1(u_2)$$

$$\alpha_0 = H_0(y_2)\, W_0(v_2, w_2) - F\, H_1(y_2)\, L_0(w_2, v_2)$$

$$\beta_0 = H_0(y_2)\, L_1(v_2, w_2) - F\, H_1(y_2)\, W_0(w_2, v_2)$$

$$\gamma_0 = -J_1(u_2)\, L_0(v_2, x_2) + E\, J_0(u_2)\, W_0(x_2, v_2)$$

$$\gamma_1 = J_1(u_2)\, W_0(v_2, x_2) - E\, J_0(u_2)\, L_1(x_2, v_2)$$

$$\gamma_2 = J_1(u_2)\, V(x_2, v_2) - E\, J_0(u_2)\, U(x_2, v_2) \qquad (64)$$

$$W_0(z, \zeta) = -J_0(z)\, Y_1(\zeta) + J_1(\zeta)\, Y_0(z)$$
$$L_0(z, \zeta) = J_0(z)\, Y_0(\zeta) - J_0(\zeta)\, Y_0(z)$$
$$L_1(z, \zeta) = J_1(z)\, Y_1(\zeta) - J_1(\zeta)\, Y_1(z)$$
$$U(z, \zeta) = J_2(z)\, Y_1(\zeta) - J_1(\zeta)\, Y_2(z)$$
$$V(z, \zeta) = J_2(z)\, Y_0(\zeta) - J_0(\zeta)\, Y_2(z)$$

(65)

$u_2 = \mathcal{K}_p r_p$, $\quad x_2 = \mathcal{K}_s h_0$

$v_2 = \mathcal{K}_s r_p$, $\quad y_2 = \mathcal{K}_f r_s$

$w_2 = \mathcal{K}_s r_s$ $\quad$ z and ζ are dummy variables (66)

$$W_1 = (c_0/c_p)^2 \left[1 - c_0/c_f\,(M_p - M_f)\cos\theta\right]^2$$

$$W_2 = (c_0/c_s)^2 \left[1 - c_0/c_f\,(M_s - M_f)\cos\theta\right]^2$$

$$M_1 = \left[W_1 - (c_0/c_f \cos\theta)^2\right], \quad M_2 = \left[W_2 - (c_0/c_f \cos\theta)^2\right]$$

$$E = \frac{M_2}{M_1}\frac{W_1}{W_2}, \quad F = \frac{W_2}{M_2}\, c_0/c_f \sin\theta$$

$$Q_2 = 1 - c_0/c_f\,(M_c - M_f)\cos\theta$$

$$kr_p = St_2 \left[\frac{\pi \bar{M}}{Q_2\, \Gamma^{1/2}\,(1+\Sigma)^{1/2}}\right] = \lambda_{1s},$$

$$kr_s = \lambda_{1s}\,(1+\Sigma)^{1/2} = \lambda_{2s}, \quad kr_0 = (\lambda_{1s} + \lambda_{2s})/2 = \lambda_{3s}$$

$$St_2 = \left(\frac{\omega}{2\pi}\,\frac{D}{U_m}\right)\left(\frac{U_s}{U_p}\right)^{1/2} Q_2, \quad D = 2r_s$$

$$\bar{M} = \left[\frac{M_p^2}{1+\Sigma}\,\frac{1}{P_1} + \frac{M_s^2\,\Sigma}{1+\Sigma}\,\frac{1}{P_2}\right]^{1/2} = U_m/c_0$$

$$\Gamma = \frac{U_s}{U_p}, \quad \Sigma = \frac{\pi(r_s^2 - r_p^2)}{\pi r_p^2}; \quad P_1 = \rho_0/\rho_p, \quad P_2 = \rho_0/\rho_s, \quad \rho_f \simeq \rho_0 \tag{67}$$

The symbol Γ represents the outer-to-inner (also called the secondary-to-primary) velocity ratio, and the symbol Σ represents the outer-to-inner area ratio. U_m is a chacteristic mean velocity which is obtained from conservation of momentum equation for the coaxial jet and $\bar{M}$ is its corresponding Mach number defined with respect to c_0; St_2 is the source Strouhal number observed in a frame of reference convected at a Mach number $(M_c - M_f)c_0/c_f$

and is related to the observed Strouhal number by a Doppler factor $[1-c_0/c_f (M_c - M_f) \cos\theta]$. This is also called the Doppler-corrected Strouhal number. The Doppler-corrected Strouhal number is introduced because we are considering the source convection in a frame of reference moving with flight velocity in the simulated environment. This provides relative velocity between the nozzle and the observer which is actually the case in the real situation (where the nozzle moves and the observer is static).

If we divide the right hand side of equation (63) by $\rho_f c_f$, we will get the far-field intensity properly defined, otherwise it is, strictly speaking, the circumferential average of the mean square pressure due to the contribution of all the quadrupole components of the ring source in the cold secondary stream. To get the exact far field intensity, we must now take into consideration the intensity of radiation due to the ring source in the cold primary flow. This is obtained in exactly the same way as we have done for the ring soure in the cold secondary stream. However, we will give a brief outline that leads to its final radiation result, in our next section.

4. FAR-FIELD INTENSITY DUE TO THE RING-SOURCE IN THE PRIMARY STREAM

As we have indicated earlier, the noise sources which arise as a result of the interaction due to the primary and the secondary flows is represented by considering a ring source convecting in the midst of the primary flow. The general motions of acoustic propagation are governed by the following equations:

$$\left[\frac{1}{c_p^2}\left(\frac{D}{Dt}\right)_p^2 - \nabla^2\right] p = q_m L_j \left\{\frac{\delta(r-r_0)}{r}\,\delta(z-U_c t)\, e^{i(m\phi-\omega t)}\right\}, \quad (68)$$

$$(0 \leq r \leq r_p)$$

$$\left[\frac{1}{c_s^2}\left(\frac{D}{Dt}\right)_s^2 - \nabla^2\right] p = 0 \quad , \quad (r_p \leq r \leq r_s) \tag{69}$$

$$\left[\frac{1}{c_f^2}\left(\frac{D}{Dt}\right)_f^2 - \nabla^2\right] p = 0 \, , \quad (r_s \leq r) \tag{70}$$

where we have considered, for convenience, the ring source to be convecting at a radial distance of $r = r_0$ from the axis of the flow. Following the steps as in section 3, equations (68-70) can be made to yield:

$$\left(\frac{\partial^2}{\partial r^2} + \frac{1}{r}\frac{\partial}{\partial r} + K_p^2 - \frac{m^2}{r^2}\right)\tilde{p} = q_m \frac{\delta(r-r_0)}{2\pi r} K_j(k_3) \, , \text{ for } 0 \leq r \leq r_p \tag{71}$$

$$\left(\frac{\partial^2}{\partial r^2} + \frac{1}{r}\frac{\partial}{\partial r} + K_s^2 - \frac{m^2}{r^2}\right)\tilde{p} = 0 \quad , \text{ for } \quad r_p \leq r \leq r_s \tag{72}$$

$$\left(\frac{\partial^2}{\partial r^2} + \frac{1}{r}\frac{\partial}{\partial r} + K_f^2 - \frac{m^2}{r^2}\right)\tilde{p} = 0 \, , \text{ for } \quad r_s \leq r \tag{73}$$

where

$$\left.\begin{aligned} K_p^2 &= (c_0/c_p)^2\left[k + (M_c - M_p)k_3\right]^2 - k_3^2 \\ K_s^2 &= (c_0/c_s)^2\left[k + (M_c - M_s)k_3\right]^2 - k_3^2 \\ K_f^2 &= (c_0/c_f)^2\left[k + (M_c - M_f)k_3\right]^2 - k_3^2 \end{aligned}\right\} \tag{74}$$

$$\left.\begin{aligned} &K_1 = -1, \quad K_2 = i c_0\left[k + (M_c - M_p)k_3\right] \\ &K_3 = -ik_3, \quad K_4 = k_3^2; \quad k = \omega/c_0, \quad M_c = U_c/c_0 \end{aligned}\right\} \tag{75}$$

Equations (71-73) are subject to the boundary conditions: (i) the continuity of acoustic pressure and (ii) the continuity of normal particle displacement across the boundaries at $r = r_p$ and $r = r_s$. The latter condition is expressed through the equations:

$$\left(\rho_p/\rho_s\right)\left[\frac{k+(M_c-M_p)k_3}{k+(M_c-M_s)k_3}\right]^2\left(\frac{\partial\tilde{p}}{\partial r}\right)_{r_p(+)} = \left(\frac{\partial\tilde{p}}{\partial r}\right)_{r_p(-)} \tag{76}$$

$$\left(\rho_s/\rho_f\right)\left[\frac{k+(M_c-M_s)k_3}{k+(M_c-M_f)k_3}\right]^2\left(\frac{\partial\tilde{p}}{\partial r}\right)_{r_s(+)} = \left(\frac{\partial\tilde{p}}{\partial r}\right)_{r_s(-)} \tag{77}$$

Now making use of the general solutions for equations (71-73) and the above boundary conditions, one can find the far field solution through the method of stationary phase as:

$$p(R,\theta,\phi,t) = \frac{2q_m}{i\pi^2 r_s r_p}\,\frac{K_j(k_3)_0\,J_m(K_p r_0)}{G_m R}\cdot\frac{\exp i\{Rk\,c_0/c_f - \omega t + m(\phi-\pi/2)}{\left[1-c_0/c_f(M_c-M_f)\cos\theta\right]} \tag{78}$$

where

$$G_m = G_{fs}(H_m,J_m)\,G_{sp}(Y_m,J_m) - G_{fs}(H_m,Y_m)\,G_{sp}(J_m,J_m) \tag{79}$$

$$G_{sp}(Y_m,J_m) = K_s\Lambda_{ps}Y_m'(K_s r_p)\,J_m(K_p r_p) - K_p Y_m(K_s r_p)\,J_m'(K_p r_p) \tag{80}$$

$$G_{sp}(J_m,J_m) = K_s\Lambda_{ps}J_m'(K_s r_p)\,J_m(K_p r_p) - K_p J_m(K_s r_p)\,J_m'(K_p r_p) \tag{81}$$

$$G_{fs}(H_m, J_m) = K_f \Lambda_{sf} H_m'(K_f r_s) J_m(K_s r_s) - K_s H_m(K_f r_s) J_m'(K_s r_s) \quad (82)$$

$$G_{fs}(H_m, Y_m) = K_f \Lambda_{sf} H_m'(K_f r_s) Y_m(K_s r_s) - K_s H_m(K_f r_s) Y_m'(K_s r_s) \quad (83)$$

$$K_p = \frac{k}{1 - c_0/c_f (M_c - M_f)\cos\theta} \left\{ (c_0/c_p)^2 \left[1 - c_0/c_f (M_p - M_f)\cos\theta \right]^2 - (c_0/c_f \cos\theta)^2 \right\}^{1/2}$$

$$K_s = \frac{k}{1 - c_0/c_f (M_c - M_f)\cos\theta} \left\{ (c_0/c_s)^2 \left[1 - c_0/c_f (M_s - M_f)\cos\theta \right]^2 \right.$$

$$K_f = \frac{k\, c_0/c_f \sin\theta}{1 - c_0/c_f (M_c - M_f)\cos\theta}$$

$$(k_3)_0 = \frac{k\, c_0/c_f \cos\theta}{1 - c_0/c_f (M_c - M_f)\cos\theta} \quad (84)$$

$$\left.\begin{aligned} \Lambda_{ps} &= \nu_{ps} \\ \Lambda_{sf} &= \nu_{sf} \end{aligned}\right\} \quad (85)$$

$$K_1 = -1$$

$$K_2 = i c_0 k \frac{1 - c_0/c_f (M_p - M_f)\cos\theta}{1 - c_0/c_f (M_c - M_f)\cos\theta}$$

$$K_3 = -ik \frac{c_0/c_f \cos\theta}{1 - c_0/c_f (M_c - M_f)\cos\theta}$$

$$K_4 = \frac{\left(k\, c_0/c_f\right)^2 \cos^2\theta}{\left[1 - c_0/c_f\left(M_c - M_f\right)\cos\theta\right]^2}$$

(86)

Here R is the distance between the center of the ring source in the primary flow and the observer's location, and θ is the angle made by this line with the directon of source convection, all considered at the time of emission. It has to be noted here that only when the centers of the ring sources in the primary flow and the secondary flow coincide, their distances from the observer as well as their angles will be the one and the same, i.e. only then $R = \mathcal{R}$, and θ's in both cases become the same.

To predict the intensity of radiation due to a ring source in the primary stream, we follow the procedure outlined in section (3.3) where we considered a similar case for a ring source in the secondary stream. Making use of the equation (78) for an axisymmetric ring source without any periodicity m along ϕ, and differentiating the simple source result with respect to the source coordinate at $r = r_0$, we get

$$\left(\frac{\partial p}{\partial r}\right)_{r_0} = -\frac{2\rho_p K_p K_1}{i\pi^2 r_s r_p} \frac{J_1(K_p r_0)}{G_0} \frac{\exp i\{Rk\, c_0/c_f - \omega t\}}{R\left[1 - c_0/c_f\left(M_c - M_f\right)\cos\theta\right]} \qquad (87)$$

$$\left(\frac{\partial^2 p}{\partial r^2}\right)_{r_0} = -\frac{2\rho_p K_p^2 K_1}{i\pi^2 r_s r_p} \frac{\left[J_0(K_p r_0) - J_2(K_p r_0)\right]}{G_0} \frac{\exp i\{Rk\, c_0/c_f - \omega t\}}{R\left[1 - c_0/c_f\left(M_c - M_f\right)\cos\theta\right]} \qquad (88)$$

$$\left(\frac{\partial^2 p}{\partial x \partial z}\right)_{r_0} = -\frac{2\rho_p K_p K_3}{i\pi^2 r_s r_p}\,\frac{J_1(K_p r_0)}{G_0}\,\frac{\exp i\{Rk\,c_0/c_f - \omega t\}}{R[1 - c_0/c_f(M_c - M_f)\cos\theta]} \tag{89}$$

where

$$G_0 = G_{fs}(H_0, J_0)\,G_{sp}(Y_0, J_0) - G_{fs}(H_0, Y_0)\,G_{sp}(J_0, J_0) \tag{90}$$

and the expressions for G_{fs} (H_0, J_0), $G_{sp}(Y_0, J_0)$, etc. are obvious in equations (80-83) from which we can easily derive them by putting m = 0. It may be noted here that the strength of the ring source in the primary flow has been replaced by the density ρ_p of the primary flow, since they are directly related. Mani and Balsa have successfully introduced this direct relationship between the source strength and the fluid density in almost all of their works on jet noise.

To obtain the individual far-field radiation contribution due to all the fundamental quadrupole components of an axisymmetric ring source devoid of any periodicity m along ϕ, we make use of the coordinate relations in (61) as well as the relations in equations (78, and 87-89) which yield:

$$b_{11} = \frac{2}{G_0}\,\frac{\rho_p K_p}{i\pi^2 r_s r_p r_0}\left[\frac{K_p r_0}{2}\left\{J_0(K_p r_0) - J_2(K_p r_0)\right\}\cos^2\phi + \sin^2\phi\; J_1(K_p r_0)\right]\cdot \frac{\exp i\{Rk\,c_0/c_f - \omega t\}}{R[1 - c_0/c_f(M_c - M_f)\cos\theta]}$$

$$b_{22} = \frac{2}{G_0}\,\frac{\rho_p K_p}{i\pi^2 r_s r_p r_0}\left[\frac{K_p r_0}{2}\left\{J_0(K_p r_0) - J_2(K_p r_0)\right\}\sin^2\phi + \cos^2\phi\; J_1(K_p r_0)\right]\cdot \frac{\exp i\{Rk\,c_0/c_f - \omega t\}}{R[1 - c_0/c_f(M_c - M_f)\cos\theta]}$$

$$b_{33} = \frac{2}{G_0}\,\frac{\rho_p (k\,c_0/c_f)^2 \cos^2\theta}{i\pi^2 r_s r_p}\,J(K_p r_0)\,\frac{\exp i\{Rk\,c_0/c_f - \omega t\}}{R[1 - c_0/c_f(M_c - M_f)\cos\theta]^3}$$

$$b_{12} = \frac{2}{G_0}\,\frac{\rho_p K_p}{i\pi^2 r_s r_p r_0}\left[\frac{K_p r_0}{2}\left\{J_0(K_p r_0) - J_2(K_p r_0)\right\} - J_1(K_p r_0)\right]\sin\phi\cos\phi\,.\,\frac{\exp i\{Rk c_0/c_f - \omega t\}}{R\left[1 - c_0/c_f (M_c - M_f)\cos\theta\right]}$$

$$b_{13} = \frac{2}{G_0}\,\frac{\rho_p K_p}{\pi^2 r_s r_p}\left(k\, c_0/c_f \cos\theta\cos\phi\right) J_1(K_p r_0)\,\frac{\exp i\{Rk c_0/c_f - \omega t\}}{R\left[1 - c_0/c_f (M_c - M_f)\cos\theta\right]^2}$$

$$b_{23} = \frac{2}{G_0}\,\frac{\rho_p K_p}{\pi^2 r_s r_p}\left(k\, c_0/c_f \cos\theta\,\sin\phi\right) J_1(K_p r_0)\,\frac{\exp i\{Rk c_0/c_f - \omega t\}}{R\left[1 - c_0/c_f (M_c - M_f)\cos\theta\right]^2} \qquad (91)$$

Using the above relations in equation (54), and making use of the radiation formula given in equation (53), one finds the intensity for a far-field radiation as:

$$I_{rcp} = \langle \bar{b}_{33}^2 \rangle + 2\langle \bar{b}_{11}^2 \rangle + 2\langle \bar{b}_{12}^2 \rangle + 4\langle \bar{b}_{13}^2 \rangle$$

$$= \left(\frac{2\rho_p}{\pi^2 R r_s r_p}\right)^2 \frac{1}{|M_2 \delta_1|^2}\left\{\frac{(c_0/c_f)^4 \cos^4\theta}{Q_1^2}\left|\frac{J_0(x_1)}{M_1}\right|^2\right.$$

$$+ \frac{1}{\lambda_{3p}^2}\left|\frac{3}{16}x_1^2\left\{J_0(x_1) - J_2(x_1)\right\}^2 + \frac{3}{4}\left\{J_1(x_1)\right\}^2 + \frac{x_1 J_1(x_1)}{4}\left\{J_0(x_1) - J_2(x_1)\right\}\right|$$

$$+ \frac{1}{\lambda_{3p}^2}\left|\frac{x_1^2}{16}\left\{J_0(x_1) - J_2(x_1)\right\}^2 + \frac{1}{4}\left\{J_1(x_1)\right\}^2 - \frac{x_1 J_1(x_1)}{4}\left\{J_0(x_1) - J_2(x_1)\right\}\right|$$

$$\left. + \frac{2(c_0/c_f)^2 \cos^2\theta}{Q_1^2}\left|J_1(x_1)\right|^2\right\} \qquad (92)$$

where

$$\delta_1 = E\beta\; J_0(u_1) + \alpha\, J_1(u_1)$$

$$\alpha = H_0(y_1)\, W_0(v_1, w_1) - F\, H_1(y_1)\, L_0(w_1, v_1)$$

$$\beta = H_0(y_1)\, L_1(v_1, w_1) - F\, H_1(y_1)\, W_0(w_1, v_1) \qquad (93)$$

$$u_1 = K_p r_p, \qquad x_1 = K_p r_o$$
$$v_1 = K_s r_p, \qquad y_1 = K_f r_s$$
$$w_1 = K_s r_s \tag{94}$$

$$Q_1 = 1 - \omega/c_f (M_c - M_f) \cos\theta$$
$$kr_p = St_1 \left[\frac{\pi \bar{M}}{Q_1 \Gamma^{1/2} (1+\Sigma)^{1/2}} \right] = \lambda_{1p}$$
$$kr_s = \lambda_{1p} (1+\Sigma)^{1/2} = \lambda_{2p}$$
$$kr_o = \lambda_{1p}/2 = \lambda_{3p}$$
$$St_1 = \left(\frac{\omega}{2\pi} \frac{D}{U_m} \right) \left(\frac{U_s}{U_p} \right)^{1/2} Q_1 \tag{95}$$

As before, St_1 is the Source-Strouhal number where the source is moving with a Mach number $(M_c - M_f)\, c_o/c_f$ in a frame of reference moving with flight velocity in the simulated environment. The notation I_{rcp} in equation (92) is introduced to signify that it implies the intensity due to radiation from a ring-source in the cold primary stream.

5. INTENSITY OF RADIATION DUE TO RING SOURCES IN COLD COAXIAL DUAL FLOW AND APPLICATION OF THE THEORY

Since the problem under consideration is a linear one, the effective radiation due to the coaxial dual flow phenomenom will be considered as the linear combination of the two radiation fields generated by the ring-sources in the primary flow as well as in the secondary flow. In view of this superposition of the two fields, the intensity of radiation in far-field due to the

coaxial dual flow is given as the combined effects of the intensities given in equations (63) and (92). This is expressed as:

$$I=\left(\rho_f/R\right)\frac{64\left(1+\Sigma\right)}{\pi^4 D^4}\left[\frac{RCP}{P_1^2}+\left(\frac{\pi}{1+\sqrt{1+\Sigma}}\right)^2\frac{RCS}{P_2^2}\right] \tag{96}$$

where D is the external diameter of the coaxial jet (and is related to the internal diameter through the relation $D = d\,(1+\Sigma)^{1/2}$) and:

$$RCP=\frac{1}{\left|M_2\delta_1\right|^2}\left\{\frac{\left(c_0/c_f\right)^4\cos^4\theta}{Q_1^2}\left|\frac{J_0(\chi_1)}{M_1}\right|^2\right.$$

$$+\frac{1}{\lambda_{3p}^2}\left|\frac{3}{16}\chi_1^2\left\{J_0(\chi_1)-J_2(\chi_1)\right\}^2+\frac{3}{4}\left\{J_1(\chi_1)\right\}^2+\frac{\chi_1 J_1(\chi_1)}{4}\left\{J_0(\chi_1)-J_2(\chi_1)\right\}\right|$$

$$+\frac{1}{\lambda_{3p}^2}\left|\frac{\chi_1^2}{16}\left\{J_0(\chi_1)-J_2(\chi_1)\right\}^2+\frac{1}{4}\left\{J_1(\chi_1)\right\}^2-\frac{\chi_1 J_1(\chi_1)}{4}\left\{J_0(\chi_1)-J_2(\chi_1)\right\}\right|$$

$$\left.+\frac{2\left(c_0/c_f\right)^2\cos^2\theta}{Q_1^2}\left|J_1(\chi_1)\right|^2\right\} \tag{97}$$

$$RCS=\frac{1}{Q_2^2\left|\delta_2\right|^2}\left\{\frac{\left|\gamma_0\right|^2\lambda_{3s}^2\left(c_0/c_f\right)^4\cos^4\theta}{Q_2^2\left|M_2\right|^2}\right.$$

$$+\left|\frac{3}{16}\left\{\chi_2(\gamma_0-\gamma_2)\right\}^2+\frac{3}{4}\gamma_1^2+\frac{\chi_2\gamma_1}{4}\left(\gamma_0-\gamma_2\right)\right|$$

$$+$$

$$+\left|\frac{1}{16}\left\{\chi_2(\gamma_0-\gamma_2)\right\}^2+\frac{\gamma_1^2}{4}-\frac{\chi_2\gamma_1}{4}(\gamma_0-\gamma_2)\right|$$

$$+\frac{2|\gamma_1|^2\lambda_{3s}^2(c_0/c_f)^2\cos^2\theta}{Q_2^2}\Bigg\} \tag{98}$$

It has to be pointed out that in order to make a straightforward linear combination of the radiation effects and also to keep the involved mathematics less complicating, we have considered a situation when the centers of the ring sources perfectly coincide and as such they emit radiations which reach the observer simultaneously. In such a situation $R = \mathcal{R}$ and θ, the angle of emission at the retarded time is the same for both. This fact has been well taken care of in developing the expression for the intensity of radiation due to both the rings as given in equation (96).

In all the plots the computation is made for the directional intensity at Strouhal number, $St_1 = 0.2$, $St_2 = 0.2$, and is expressed in terms of sound pressure levels, in decibels (dB), where

$$dB = 10\ \log_{10} I(M_f) \tag{99}$$

$$I(M_f) = \frac{64}{\pi^4}(1+\Sigma)\left[\frac{RCP}{P_1^2}+\left(\frac{\pi}{1+\sqrt{1+\Sigma}}\right)^2\frac{RCS}{P_2^2}\right] \tag{100}$$

The parameteric values of $P_1 = 1 = P_2$ implies the consideration of a cold coaxial jet where $\rho_p = \rho_s = \rho_f$. Furthermore, while making computations, the convection Mach number of the ring-source in the primary flow is given by $M_c = (M_p + M_s)/2$ and the convection Mach number of the ring-source in the secondary flow is given by $\mathcal{M}_c = (M_s + M_f)/2$. The convection Mach numbers

of the ring sources are so expressed in order to reflect the speeds of the flows whose interactions are solely responsible for the generation of these sources.

With these assumptions, the change in intensity level is analyzed in figures 5-6 by a plot of variation in intensity level with direction θ measured from the direction of convection. These figures illustrate the change with Mach number M_f of the directional intensity field of two representative ring sources, one convecting in the midst of the primary flow and the other convecting in the midst of the secondary flow, at points far from them. Figure 5(b) represents a coaxial flow situation where the inner/primary flow velocity ($M_p = 0.9$) is higher than the outer/secondary flow velocity ($M_s = 0.5$) and represents a conventional cold coaxial configuration, whereas figure 5(a) represents an altogether different flow profile where the primary flow and the secondary flow are completely inverted so as to make the primary flow Mach number ($M_p = 0.5$) much less than the secondary flow Mach number ($M_s = 0.9$). This latter coaxial flow pattern is called the inverted velocity profile configuration. In both figures, one notices that as we move from a static ($M_f = 0$) to flight situation ($M_f > 0$), the intensity of radiation in the aft quadrant ($0 < \theta < \pi/2$) diminishes and the intensity of radiation in the forward quadrant ($\pi/2 < \theta < \pi$) increases. This observation suggests that as we move from the aft quadrant to the forward quadrant there is a strong preference for forward emission with increasing flight Mach number M_f. In other words, forward speed induces amplification of noise in the forward quadrant and reduction of noise in the aft quadrant. Another point of interest that attracts attention is the crossing of all the curves at the angle at $\theta = 90°$. Their coalescence at one point implies that at $\theta = 90°$,

the impact or the effects of flight are completely absent. In both these two figures, one notices that the inversion of velocities, from high-inner/low-outer to low-inner/high-outer, causes a substantial reduction of the radiation intensity at all angles. This takes place under constant thrust, and constant massflow conditions. This observation tells us that for an equal outer-to-inner area ratio ($\Sigma = 1$) and under constant thrust and constant massflow conditions, inverted velocity profile coaxial jet is quieter than a conventional velocity profile coaxial jet. This point is more explicitly illustrated in figures 6(a)-6(c) which reassert the fact that compared to a conventional profile coaxial jet, an inverted profile coaxial jet flow is much less noisy under all conditions, both statically and also in flight. Thus an inverted velocity profile seems to retain its quietening quality not only when there is no flight, but also at practically all flight conditions.

In figure 6(a) the comparison between the conventional velocity profile and the inverted profile is at constant massflow and constant thrust, at area ratio $\Sigma=1$. The noise reduction due to the inverted profile relative to the conventional profile is at least 10dB in the aft quadrant and around 16 dB in the forward quadrant. The forward quadrant noise reduction is even more as one gets closer to the jet axis in the forward direction. As one moves from the static to the flight case, the static benefit in noise reduction in the aft quadrant is diminished by nearly 1.5 dB at $M_f = 0.3$ and by 2 dB at $M_f = 0.6$, whereas that in the forward quadrant is more or less maintained. Nonetheless, as a result of flight, the overall level of SPL in the aft quadrant ($0 < \theta < /2$) is reduced and that in the forward quadrant ($\pi/2 < \theta < \pi$) is amplified. This observation is in tune with our earlier

findings where we had noted that the effects of flight induce reduction of noise in the aft quadrant and amplification of noise in the forward quadrant.

When the area ratio is increased to Σ = 4 and 10 as in figures 6(b) and 6 (c) respectively, the inverted velocity profile provides substantially higher bypass ratios and also induces increased massflow and increased thrust. This is not the case for the conventional profiles where the mass flow and thrust are substantially reduced as a result of increasing area ratio. This observation may change as we will examine the inverted profile of a hot coaxial jet flow in part 2. Comparison of all the plots of Figure (6) indicate that the attenuation obtained over all angles as a result of flow inversion is substantial when a low area ratio (and hence a low bypass ratio operation) is maintained. This observation may also suggest that a low bypass ratio operation obtainable at an outer-to-inner area ratio of Σ = 1 can be combined with an inverted velocity profile concept to achieve a really worthwhile noise suppression both statically and in flight. Figure 7 provides a visualization of the conventional profile and the inverted profile (and variable stream control engine (VSCE) cycle which we discuss in Part 2).

6. CONCLUSIONS

The problem of the effects of flight on coaxial jet noise has been studied on the basis of a simple vortex-sheet flow model. The elegance of handling the problem comes through the deliberate suppression of the flow instabilities and also through the inherent simplicity of the vortex sheet model. As a result of this study, we find that the effects of flight on noise from an unheated coaxial dual flow induce:

i) amplification of noise in the forward quadrant ($\pi/2 < \theta < \pi$)

ii) reduction of noise in the aft quadrant ($0 < \theta < \pi/2$) and

iii) absolutely no impact on noise at $\theta = 90°$ to the jet axis.

Furthermore, this study shows that:

iv) at constant massflow and thrust maintained at an outer-to-inner area ratio (Σ) equal to unity, an inverted velocity profile is at least 10 dB (SPL) quieter than a conventional profile cycle at angles in the aft quadrant and 16 dB (SPL) quieter at angles in the forward quadrant when there is no flight,

v) the static benefit in noise reduction is more or less maintained in the forward quadrant, but is somewhat lost by nearly 1.5 to 2 dB in the aft quadrant,

vi) an inverted velocity profile achieves increased massflow and thrust as the area ratio Σ increases, in contrast to the conventional profile which incurs massloss and thrustloss with the increase in area ratio,

vii) the amount of noise reduction due to an inverted velocity profile relative to a conventional profile gradually diminishes as the area ratio Σ increases, and lastly

viii) an inverted velocity profile, combined with a low bypass ratio operation obtainable at an outer-to-inner area ratio equal to unity provides the best optimization of noise while still maintaining the constant massflow and thrust in perfect parity with a conventional profile cycle.

The above conclusions are derived for an unheated coaxial dual flow and may change when we analyze the effects of flight on noise from a heated coaxial dual flow (in part 2).

REFERENCES

BALSA, T.F. & GLIEBE, P.R. 1977 Aerodynamics and noise of coaxial jets. AIAA Journal 15, 1550-1558.

CROW, S.C. & CHAMPAGNE, F.H. 1971 Orderly structures in jet turbulence. J. Fluid Mech. 48, 547-591.

DASH, R. 1978 Analysis of flight effects on noise radiation from jet flow using a convecting quadrupole model. AIAA paper no. 78-192.

DASH, R. 1979a Analysis of flight effects on noise radiation from dual-flow coaxial jets. AIAA paper no. 79-06109.

DASH, R. 1979b Effects of forward velocity on sound radiation from convecting monompole and dipole sources in jet flow. J. Sound and Vib. 64, 187-207.

FFOWCS WILLIAMS, J.E. 1977 Aeroacoustics. Ann Rev. Fluid Mech. 9, 447-468.

GOLDSTEIN, M.E. & HOWES, W.L. 1973 New aspects of subsonic aerodynamic noise theory. NASA Technicla Note D-7158.

HARDIN, J.C. 1974 Noise produced by the large-scale transition region structure of turbulent jets. AIAA paper no. 74-550.

LILLEY, G.M 1972 The generation and radiation of supersonic jet noise, vol IV. AFAPL-TR-72-53.

MANI, R. 1972 A moving source problem relevant to jet noise. J. Sound and Vib. 25, 337-347.

MANI, R. 1974 Further studies on moving source solutions Relevant to jet noise. J. Sound and Vib. 35, 101-117.

MANI, R. 1976a The influence of jet flow on jet noise. Part 1. The noise of unheated jets. J. Fluid Mech. 73, 753-778.

MANI R. 1976b The influence of jet flow on jet noise. Part 2. The noise of heated jets. J. Fluid Mech. 73, 779-793.

PHILLIPS, O.M. 1960 On the generation of sound by supersonic turbulent shear layers. J. Fluid Mech. 9, 1-28.

RIBNER, H.S. 1969 Quadrupole correlations governing the pattern of jet noise. J. Fluid Mech. 38, 1-24.

SCHARTON, T.D., WHITE, P.H. & RENTZ, P.E. et. al. 1972 Investigation of supersonic jet noise using jet fluctuating pressure probes. BBN Report no. 2220.

WOOLDRIDGE, C.E. & WOOTEN, D.C. 1971 A study of the large-scale eddies of jet turbulence producing jet noise. AIAA paper no. 71-154.

FIGURE CAPTIONS

Figure 1. Practical configuration of the model.

Figure 2. Flight simulation of the model.

Figure 3. Retarded coordinates and emission from ring-source in the secondary stream

Figure 4. Periodicity of the ring-source along ϕ (occurs in the form of $e^{in\phi}$)

Figure 5. Change in directional intensity as a result of flight at an outer-to-inner area ratio $\Sigma = 1$.

a) inverted velocity profile, $M_p = 0.5$, $M_s = 0.9$

b) conventional profile, $M_p = 0.9$, $M_s = 0.5$

Figure 6(a). Comparison of SPL due to conventional profile (CP) and inverted profile (IP) at constant massflow and thrust, and area ratio $\Sigma = 1$.

CP(●): $M_p = 0.9$, $M_s = 0.5$, $\bar{M} = 0.73$

IP(⊙): $M_p = 0.5$, $M_s = 0.9$, $\bar{M} = 0.73$

Figure 6(b). Comparison of SPL due to conventional profile (CP) and inverted profile (IP) at unequal massflow and thrust, and area ratio $\Sigma = 4$.

CP(●): $M_p = 0.9$, $M_s = 0.5$, $\bar{M} = 0.60$

IP(⊙): $M_p = 0.5$, $M_s = 0.9$, $\bar{M} = 0.84$

Figue 6(c) Comparison of SPL due to conventional profile (CP) and inverted profile (IP) at unequal massflow and thrust, and area ratio $\Sigma = 10$.

CP(●): $M_p = 0.9$, $M_s = 0.5$, $\bar{M} = 0.55$

IP(⊙): $M_p = 0.5$, $M_s = 0.9$, $\bar{M} = 0.87$

Figure 7. Different engine cycles of a coaxial flow.

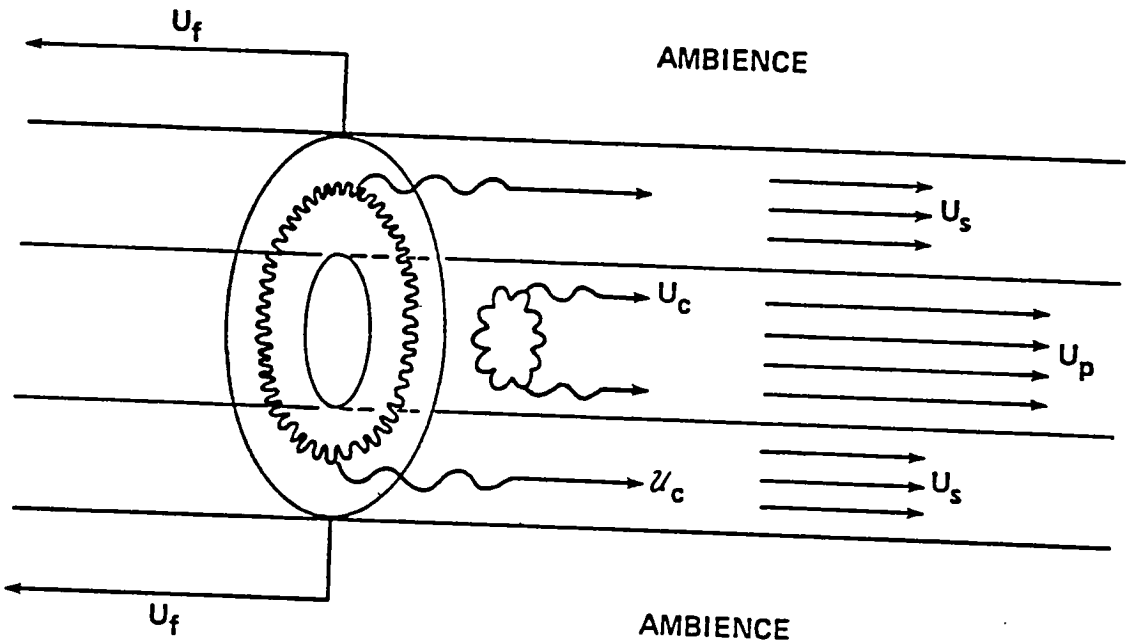

Figure 1

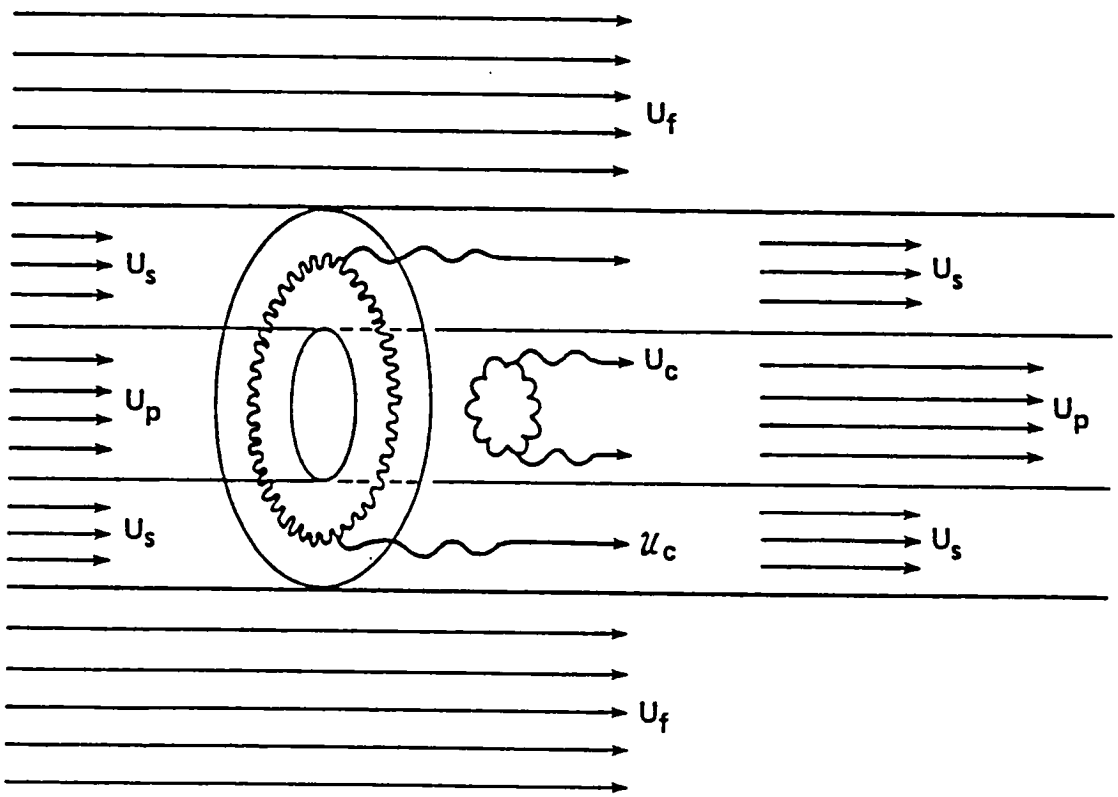

Figure 2

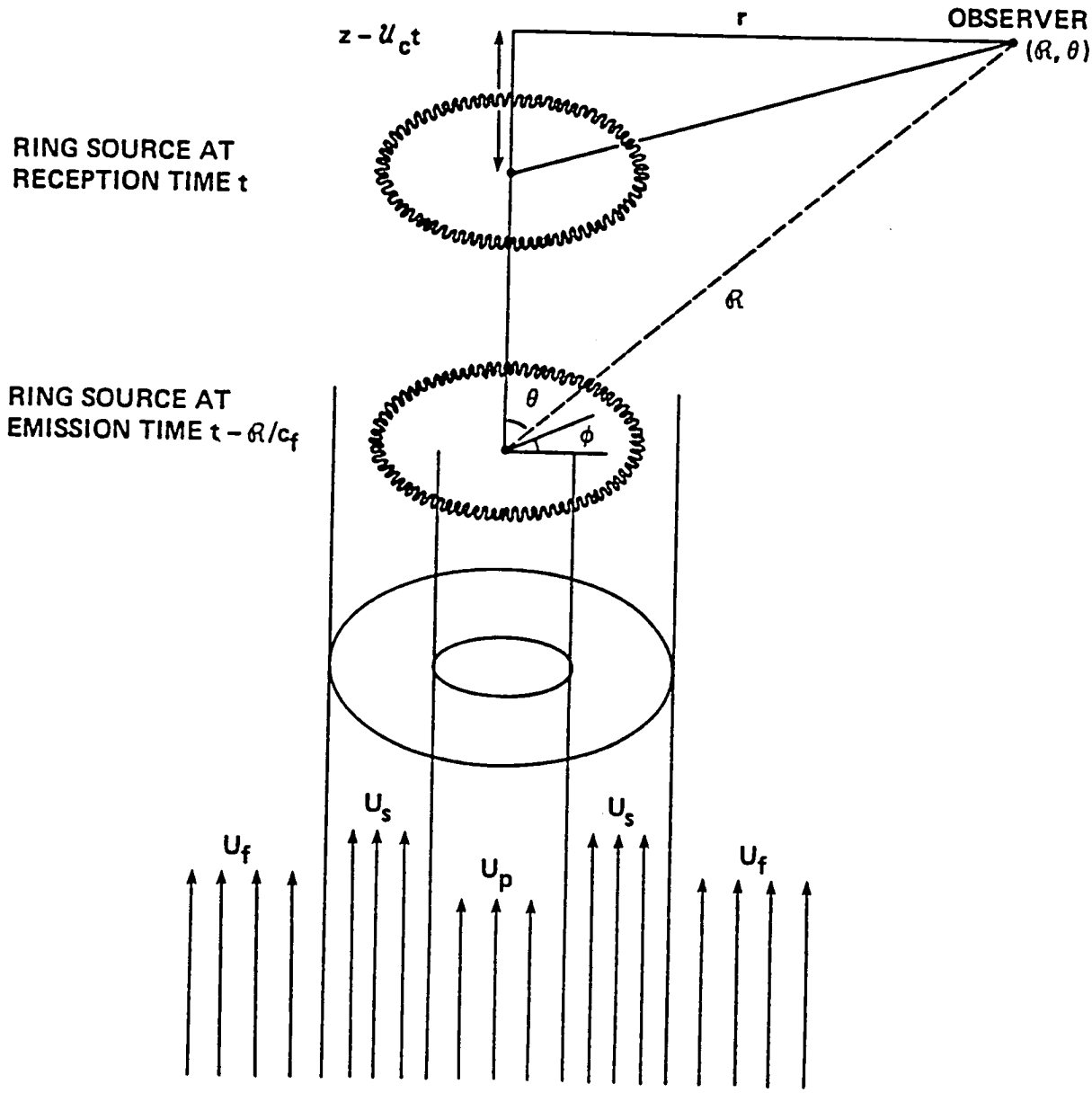
z - U_ct
r
OBSERVER
(R, θ)
RING SOURCE AT
RECEPTION TIME t
R
RING SOURCE AT
EMISSION TIME t - R/c_f
θ
ϕ
U_f
U_s
U_p
U_s
U_f

Figure 3

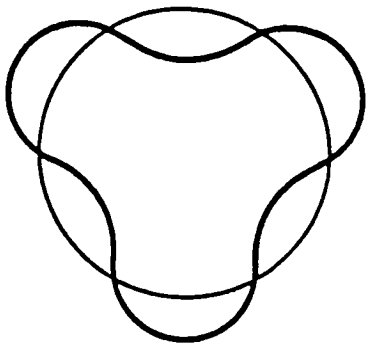

n = 3

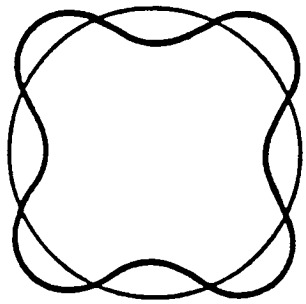

n = 4

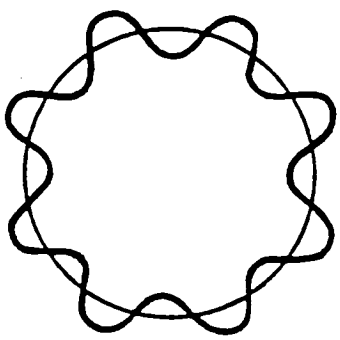

n = 8

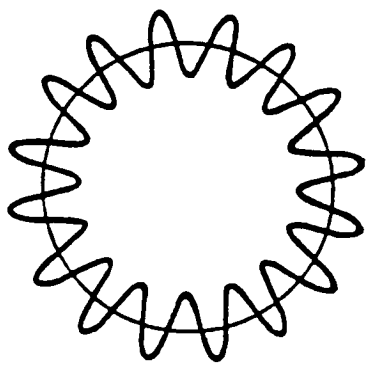

n = 16

Figure 4

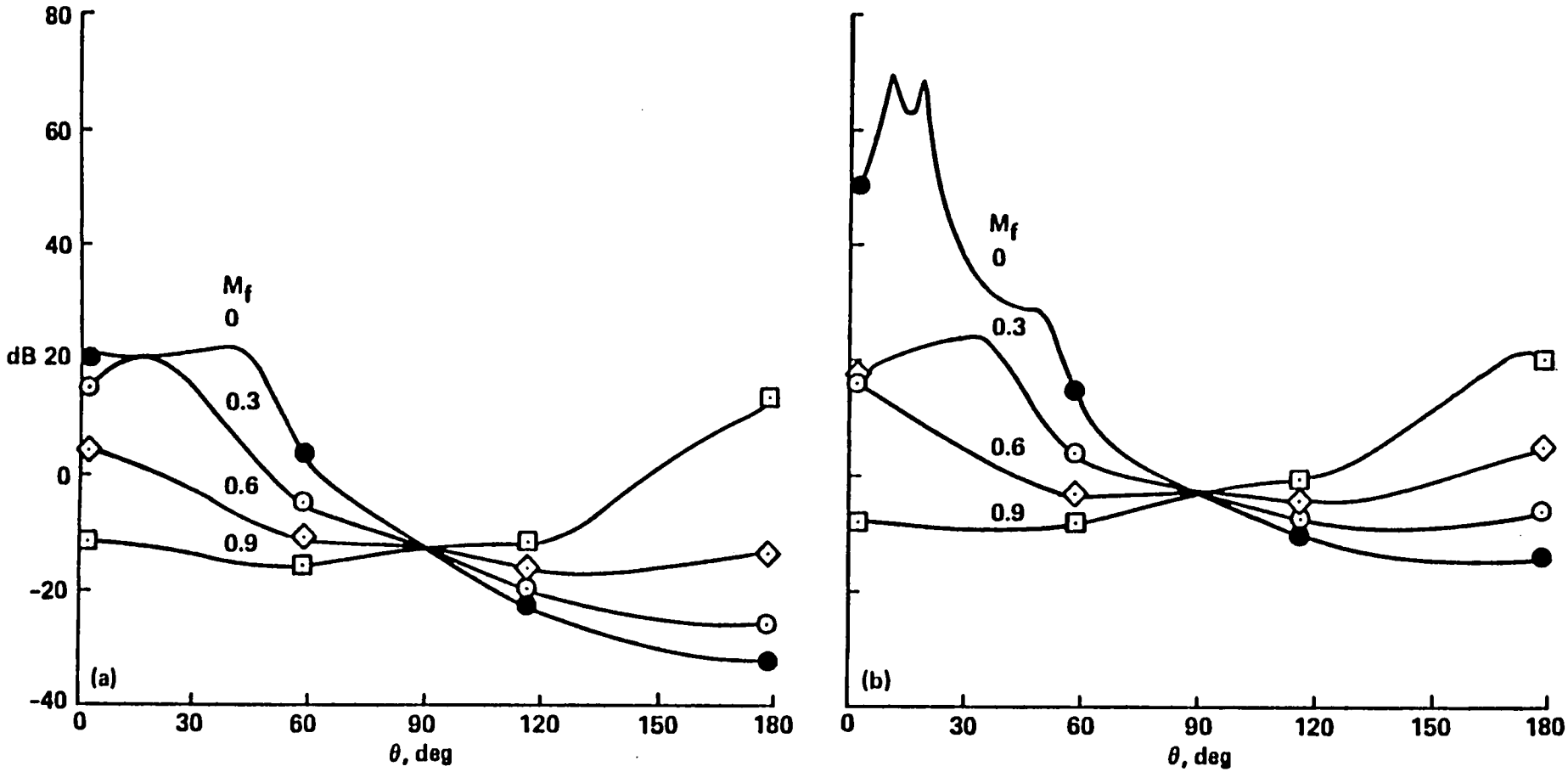
80
60
40
dB 20
0
-20
-40
M_f
0
0.3
0.6
0.9
(a)
0
30
60
90
120
150
180
θ, deg
M_f
0
0.3
0.6
0.9
(b)
0
30
60
90
120
150
180
θ, deg

Figure 5 (a) & (b)

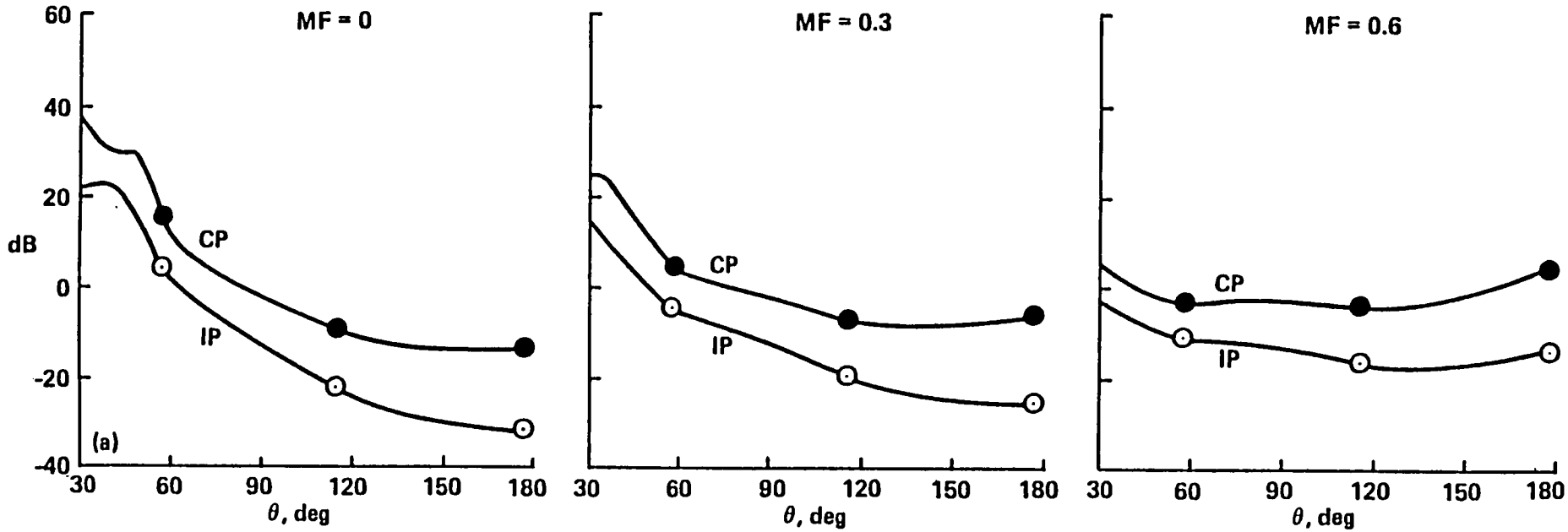

Figure 6 (a)

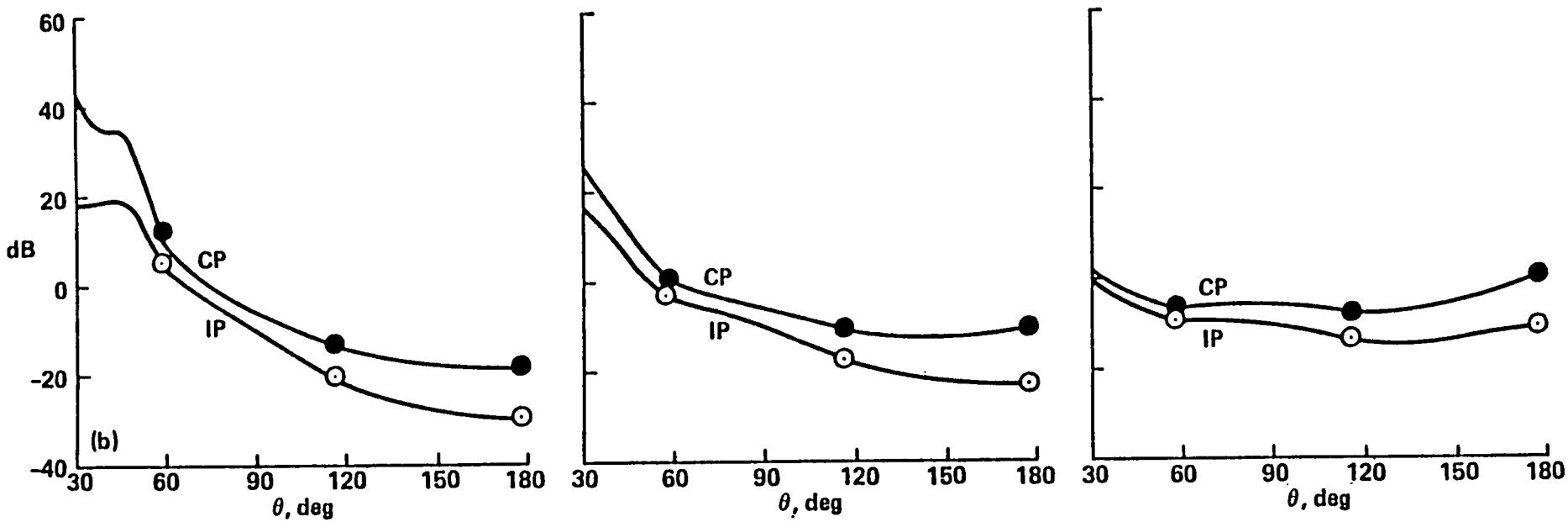
60
40
20
dB
0
-20
-40
(b)
CP
IP
30
60
90
120
150
180
θ, deg
CP
IP
30
60
90
120
150
180
θ, deg
CP
IP
30
60
90
120
150
180
θ, deg

Figure 6 (b)

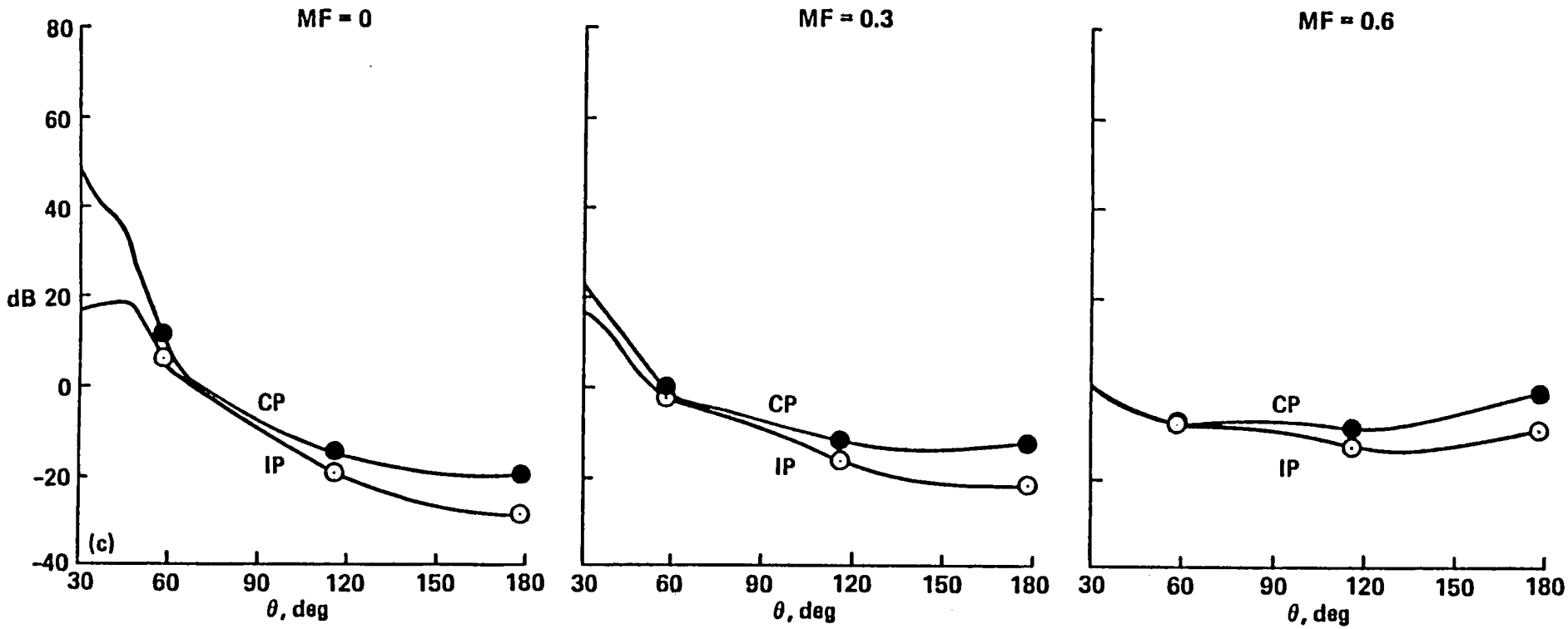
MF = 0
MF = 0.3
MF = 0.6
80
60
40
dB 20
0
-20
-40
CP
IP
(c)
30
60
90
120
150
180
θ, deg

Figure 6 (c)

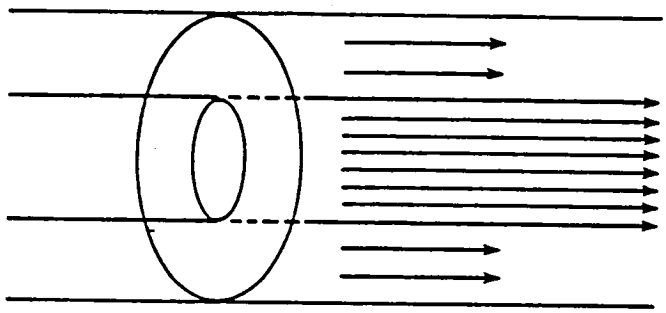

CONVENTIONAL PROFILE

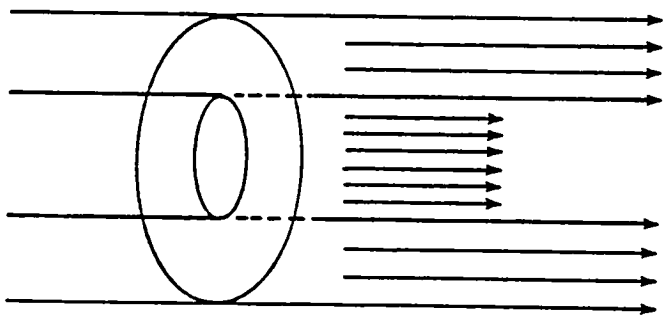

INVERTED PROFILE

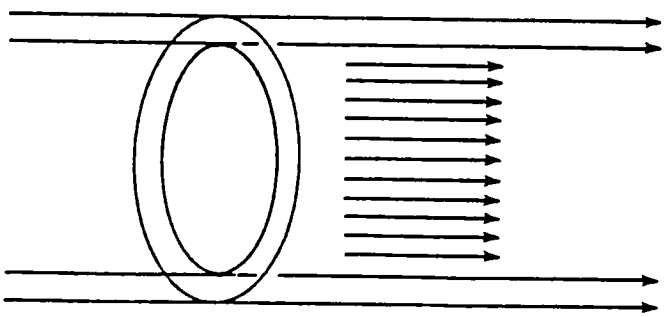

VSCE-CYCLE

Figure 7